INSTITUTE OF PHYSICS PUBLISHING PLASMA SOURCES SCIENCE AND TECHNOLOGY

Plasma Sources Sci. Technol. **15** (2006) S148–S168 doi:10.1088/0963-0252/15/4/S02

Application of mid-infrared tuneable diode laser absorption spectroscopy to plasma diagnostics: a review

J Röpcke[1,5], G Lombardi[2], A Rousseau[3] and P B Davies[4]

[1] INP-Greifswald, 17489 Greifswald, Friedrich-Ludwig-Jahn-Str. 19, Germany
[2] CNRS LIMHP, Université Paris XIII, 99, av. J.B. Clément, 93430 Villetaneuse, France
[3] Laboratoire de Physique et Technologie des Plasmas, Ecole Polytechnique, CNRS, 91128 Palaiseau, France
[4] Department of Chemistry, University of Cambridge, Lensfield Road, Cambridge CB2 1EW, UK

E-mail: roepcke@inp-greifswald.de

Received 11 November 2005
Published 6 October 2006
Online at stacks.iop.org/PSST/15/S148

Abstract

Within the last decade mid-infrared absorption spectroscopy over a region from 3 to 17μm and based on tuneable lead salt diode lasers, often called tuneable diode laser absorption spectroscopy or TDLAS, has progressed considerably as a powerful diagnostic technique for *in situ* studies of the fundamental physics and chemistry in molecular plasmas. The increasing interest in processing plasmas containing hydrocarbons, fluorocarbons, organo-silicon and boron compounds has led to further applications of TDLAS because most of these compounds and their decomposition products are infrared active. TDLAS provides a means of determining the absolute concentrations of the ground states of stable and transient molecular species, which is of particular importance for the investigation of reaction kinetic phenomena. Information about gas temperature and population densities can also be derived from TDLAS measurements. A variety of free radicals and molecular ions have been detected by TDLAS. Since plasmas with molecular feed gases are used in many applications such as thin film deposition, semiconductor processing, surface activation and cleaning, and materials and waste treatment, this has stimulated the adaptation of infrared spectroscopic techniques to industrial requirements. The recent development of quantum cascade lasers (QCLs) offers an attractive new option for the monitoring and control of industrial plasma processes. The aim of the present paper is threefold: (i) to review recent achievements in our understanding of molecular phenomena in plasmas, (ii) to report on selected studies of the spectroscopic properties and kinetic behaviour of radicals and (iii) to describe the current status of advanced instrumentation for TDLAS in the mid-infrared.

(Some figures in this article are in colour only in the electronic version)

1. Introduction

Low-pressure, non-equilibrium molecular plasmas are of increasing interest not only in fundamental research but also in plasma processing and technology. Molecular plasmas are used in a variety of applications such as thin film deposition, semiconductor processing, surface activation and cleaning, and in materials and waste treatment. The investigation of plasma physics and chemistry *in situ* requires detailed knowledge of plasma parameters, which can be obtained by appropriate diagnostic techniques. The need for a better scientific understanding of plasma physics and chemistry has stimulated the improvement of established diagnostic techniques and the introduction of new ones. Methods based on traditional spectroscopy have now become amongst the most important.

[5] Author to whom any correspondence should be addressed.

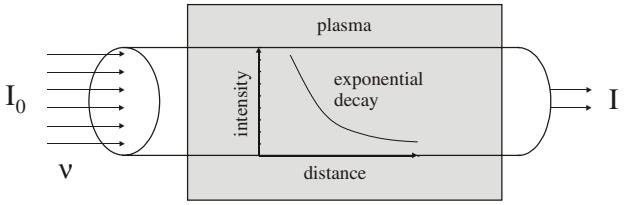

Figure 1. Absorption of external radiation in a plasma according to the Beer–Lambert Law [1].

Over the past decade, several new techniques have been successfully introduced for diagnostic studies of chemically reactive plasmas in which many short-lived and stable species are produced. It has been possible to determine absolute concentrations of ground states using spectroscopy thereby providing a link with chemical modelling of the plasma. The other essential component needed to reach the objective of improved knowledge of molecular phenomena is to determine physical parameters of the plasma by an appropriate experimental methodology.

The methods of absorption spectroscopy (AS) are of great importance in plasma diagnostics because they provide a means of determining the population densities of species in both ground and excited states. The spectral line positions provide species identification while line profiles are often connected with gas temperature and relative intensities provide information about population densities. An important advantage of AS over optical emission spectroscopy (OES) methods is that only relative intensities need to be measured to determine absolute concentrations, avoiding the problems of complete instrument calibration inherent in the OES methods. Absorption spectroscopy has been applied right across the spectrum from the vacuum ultraviolet (VUV) to the far infra-red (FIR). Continuously emitting lamps (e.g. the Xe-lamp for the VIS and NIR and the D_2-lamp for the UV) and tuneable narrow-band light sources (e.g. tuneable dye lasers, diode lasers) can be used as external light sources.

In the case where an external light source has much higher intensity than that of the plasma itself, the absorption of radiation can be described by the Beer–Lambert law which is,

$$I_\nu(l) = I_\nu(0)\exp(-\kappa(\nu)l). \qquad (1)$$

$I_\nu(0)$ and $I_\nu(l)$ are the fluxes of the radiation entering and leaving the plasma, l is the length of the absorbing (homogeneous) plasma column and $\kappa(\upsilon)$ is the absorption coefficient. Figure 1 illustrates this situation [1].

A wide variety of light sources, dispersive elements, detectors and data acquisition methods can be used for absorption spectroscopy [2]. The classic dispersion experiment for measuring the density of atomic or molecular states in plasmas by AS relies on continuous light sources and a spectrograph with a suitable detector for the spectral range of interest. The Fourier transform infra-red (FTIR) technique with a Michelson interferometer also uses a continuous light source for absorption measurements. The transmitted light intensity depends on the (variable) optical path difference between the mirrors in the two interferometer arms and yields the interferogram carrying the spectroscopic information. In contrast to dispersion techniques the FTIR spectrometer

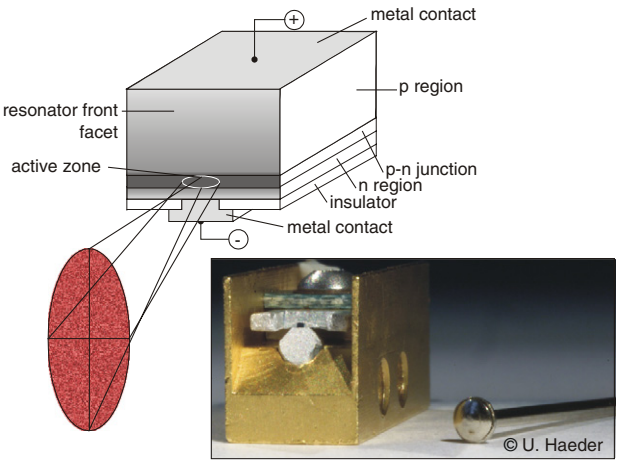

Figure 2. Schematic of the compositional structure of a lead salt diode laser and inset photograph of the laser in its packaging [1].

records the whole spectrum simultaneously (multiplex or Fellgett advantage). In principle, the resolution of FTIR can be as high as $0.002\,\mathrm{cm}^{-1}$, determined by the distance scanned by the moveable mirror, but at the expense of recording time. Fractional absorptions as small as 10^{-4} can be measured.

With the development of tuneable, narrow band light sources such as tuneable dye lasers and infrared diode lasers, these have been substituted for continuous light sources in AS experiments. These narrow band laser sources have the advantage of high spectral intensity, narrow bandwidth and continuous tuneability over the absorption profile. Figure 2 shows a homostructure lead salt diode laser used for infrared tuneable diode laser absorption spectroscopy (TDLAS) [1].

Alternatively tuneable infrared radiation can be generated using the methods of difference frequency mixing or optical parametric oscillators (OPOs). In the past these systems however had the disadvantage of rather low radiation power and were restricted to specific wavelength regions [3, 4]. New technical developments have led to solutions, which provide up to a mW of single mode power and tuneability of up to $100\,\mathrm{cm}^{-1}$ [133, 134].

Another highly sensitive novel laser technique is cavity ring-down (CRD) absorption spectroscopy. This method is based on the measurement of the intensity decay rate of a laser pulse injected into an optical cavity formed by two very highly reflective mirrors which also enclose the plasma. Absorptions as low as 10^{-9} can be measured with an acceptable signal-to-noise ratio [5]. Near infrared tuneable diode lasers have been used as the light sources for CRD spectroscopy [6]. More recently, CRD spectroscopy has been applied for density measurements of the SiH_2 radical and of nanometre sized dust particles in silane plasmas [7] and for detecting N_2^+ ions in nitrogen discharges [8].

The increasing interest in processing plasmas containing hydrocarbons, fluorocarbons or organo-silicon compounds has led to further applications of infrared AS techniques because most of these compounds and their decomposition products are infrared active. FTIR spectroscopy has been used for *in situ* studies of methane plasmas for a number of years, but it is generally insufficiently sensitive for detecting free radicals or ions in processing plasmas. TDLAS is increasingly being

used in the spectral region between 3 and 20 μm for measuring the concentrations of free radicals, transient molecules and stable products in their electronic ground states. TDLAS can also be used to measure neutral gas temperatures [9] and to investigate dissociation processes of molecular low temperature plasmas [10–13]. The main applications of TDLAS until now have been for investigating molecules and radicals in fluorocarbon etching plasmas [9, 12, 14] and in plasmas containing hydrocarbons [13, 15–21]. A wide variety of low molecular weight free radicals and molecular ions have been detected by TDLAS in purely spectroscopic studies, e.g. Si_2^- [22] and SiH_3^+ [23] in silane plasmas. Most of these spectroscopic results have yet to be applied in plasma diagnostic studies.

Molecular plasmas are increasingly being used not only for basic research but also, due to their favourable properties, for materials processing technology. These fields of application have stimulated the development of infrared spectroscopic techniques for industrial requirements. In order to exploit the capabilities of infrared TDLAS for effective and reliable on-line plasma diagnostics and process control in research and industry, compact and transportable tuneable infrared multi-component acquisition systems (IRMA, TOBI) have been developed [24, 25] (see section 4). These systems are mainly focused on (i) high speed detection of stable and transient molecular species in plasmas under non-stationary excitation conditions and (ii) on sensitive (sub-ppb) trace gas detection with the aid of multi-pass absorption cells.

The main disadvantage of TDLAS systems, based upon lead salt diode lasers, is the necessary cryogenic cooling of the lasers (and also of the detectors), because they operate at temperatures below 100 K. Systems based upon lead salt diode lasers are typically large in size and require closed cycle refrigerators and/or cryogens such as liquid nitrogen. The recent development and commercial availability of pulsed quantum cascade lasers (QCLs) offers an attractive new option for infrared absorption spectroscopy.

The present paper is intended to give an overview of recent achievements which have led to an improved understanding of phenomena in non-equilibrium molecular plasmas based on the application of TDLAS techniques. The paper is divided into three main sections: in section 2 special attention is devoted to recent studies of plasma chemistry and reaction kinetics in gas discharges containing hydrocarbons, organo-silicon and boron compounds. A link is thereby provided with chemical modelling of the plasmas. Section 3 concerns recent results of spectroscopic properties and kinetic behaviour of selected radicals, which are of special importance for reaction kinetics and chemistry in molecular processing plasmas. The current status of advanced spectroscopic instrumentation is described in section 4.

2. Plasma chemistry and reaction kinetics

2.1. General considerations

Low temperature plasmas, in particular microwave and radio frequency (RF) plasmas, have high potential for applications in plasma technology. In molecular low temperature plasmas, the species and surface conversion is frequently governed by high degrees of dissociation of the precursor molecules and the high amounts of chemically active transient and stable molecules present. For further insight into plasma chemistry and kinetics a challenging subject is to study the mainly electron induced plasma reactions leading to entire series of different chemical secondary reactions involving the whole group of substances making up the source gas molecules. Hydrocarbon precursors are of special importance, since they are used in a variety of plasma enhanced chemical vapour deposition (PECVD) processes to deposit thin carbon films. In all cases, the monitoring of transient or stable plasma reaction products, in particular the measurement of their ground state concentrations, is the key to improved understanding of fundamental phenomena in molecular non-equilibrium plasmas which can be applied in turn to many other aspects of plasma processing.

Transient molecular species, in particular radicals, influence the properties of nearly all molecular plasmas, both in the laboratory and in nature. They are of special importance in several areas of reaction kinetics and chemistry. The study of the behaviour of radicals together with their associated stable products provides a very effective approach to understand phenomena in molecular plasmas. Radicals containing carbon are of special interest for basic studies and for application in plasma technology.

Although the methyl radical (CH_3) is acknowledged to be one of the most essential intermediates in hydrocarbon plasma chemistry, only a few methods are available for its detection *in situ*. Sugai *et al* and Zarrabian *et al* employed the technique of threshold ionisation mass spectrometry to detect the methyl radical in electron cyclotron resonance plasmas containing methane [26–28]. Based on cavity ring-down spectroscopy with ultraviolet radiation CH_3 concentration measurements have been performed in a hot-filament reactor [29–31]. Most of the measurement techniques for detecting the methyl radical are based on absorption spectroscopy either with 216 nm ultraviolet radiation or in the infrared near 606 cm^{-1}. For example, the ultraviolet absorption of CH_3 at 216 nm was used for number density measurements by Child *et al* and Menningen *et al* and in different CVD diamond growth environments, hot-filament, dc and microwave plasmas [32–34]. In 2003 Lombardi *et al* performed a comparative study to detect methyl radicals using both broadband ultraviolet absorption and TDLAS [35] (see section 3.1).

The infrared TDLAS technique has proven to be highly useful because it can also be used to measure the concentrations of related species provided they are IR active. Already in 1990 Wormhoudt demonstrated this flexibility by measuring CH_3 and C_2H_2 in a CH_4–H_2 RF plasma using a long path plasma absorption cell [36]. Actually, TDLAS is probably the best method for detecting the methyl radical for several reasons. The v_2 out-of-plane bending mode is not only intense but has many lines between 600 and 650 cm^{-1}. It is then possible to derive rotational and vibrational temperatures from their relative intensities. The ($J = K$) Q-branch lines of the v_2 fundamental band near 606 cm^{-1} are particularly useful because several of them lie within 0.5 cm^{-1} of each other, i.e. within a single laser spectral mode. Rotational temperatures in the plasma are therefore easily measured from them. For more than a decade, quantifying the concentrations of methyl

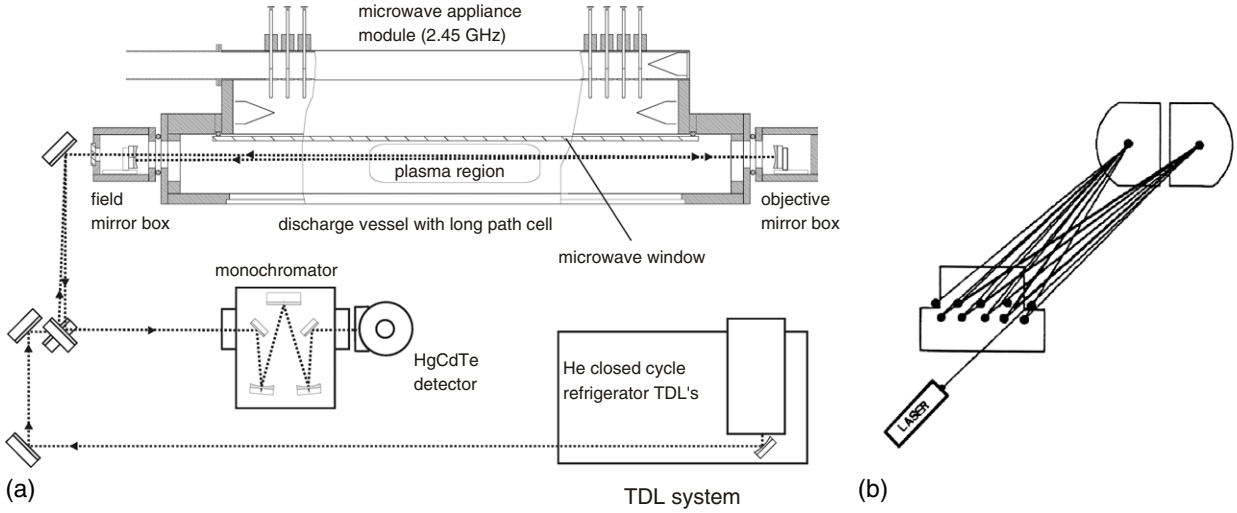

Figure 3. (*a*) Experimental arrangement of the planar microwave plasma reactor (side view) with White cell multiple pass optical arrangement and TDL infrared source. The laser beam path is indicated by dotted lines [45]. (*b*) White cell with field mirror and objective mirrors showing the laser beam path [45].

radicals via the determination of the line strength of the $Q(8, 8)$ line of methyl at 608.3 cm^{-1} by Wormhoudt and McCurdy has been highly important [37]. In 2005 using the decay of the methyl radical in the off-phase of pulsed plasmas new, precise measurements of the transition dipole moment of the υ_2 fundamental band have been performed [38] (see section 3.2).

One of the most successful applications of TDLAS is for studying the decomposition of hydrocarbons in a variety of PECVD processes. Systematic TDLAS measurements of several different hydrocarbons, including methyl, in a 20 kHz methane plasma in a parallel plate reactor were reported by Davies and Martineau [10, 39, 40]. Goto and co-workers have published numerous studies of methyl and methanol concentrations in RF and electron cyclotron resonance (ECR) plasmas under different conditions, e.g. investigating the influence of rare gases on the plasma. They have also combined IR absorption with emission spectroscopy and investigated the effect of water vapour on the methyl radical concentration in argon/methane and argon/methanol RF plasmas using TDLAS [17, 18, 41–43]. Kim *et al* measured CH_3, C_2H_2 and CH_3OH concentrations in methanol/water RF plasmas by TDLAS and found that methanol was almost completely dissociated even at medium applied power levels [44]. In 1999 a group of eleven species, CH_4, C_2H_2, C_2H_4, C_2H_6, CO, CO_2, CH_3, H_2O, CH_2O, CH_3OH, HCOOH, were detected in O_2–H_2–Ar microwave plasmas with small admixtures of methane or methanol by TDLAS [13]. Busch *et al* monitored the densities and temperatures of CH_4,O_2, CH_3, CO and CO_2 and studied aspects of the chemistry in a capacitively coupled RF discharge in 2001 [20].

2.2. Molecular microwave plasmas containing hydrocarbons

In recent years several types of microwave discharge containing hydrocarbons as precursor gases have been at the centre of interest. The most recent applications of TDLAS for plasma diagnostic purposes include studies in which many different species have been monitored under identical plasma conditions [35, 45]. These experimental data have frequently been used to model plasma chemical phenomena.

2.2.1. Studies in planar microwave reactors. In 2003 Hempel *et al* studied hydrocarbon plasmas with admixtures of nitrogen in a planar microwave reactor [46] using a tuneable diode laser (TDL) spectrometer [45]. The interest in such plasmas is based on various applications including deposition of diamond layers [47–49] and of hydrogenated carbon nitride films [50–53], detoxification of combustion gases [54], conversion to higher hydrocarbons [55], studies of astronomical objects such as interstellar clouds and stellar atmospheres [56, 57]. Such types of plasma are also gaining importance in fusion physics, since they are representative of the edge discharges observed in the proximity of the carbon surfaces of the tokamak divertors [58].

Figure 3 shows the experimental arrangement. Hempel and co-workers used TDLAS to detect the methyl radical and nine stable molecules, CH_4, CH_3OH, C_2H_2, C_2H_4, C_2H_6, NH_3, HCN, CH_2O and C_2N_2, in H_2–Ar–N_2 microwave plasmas containing up to 7% of methane or methanol, under both flowing and static conditions. The degree of dissociation of the hydrocarbon precursor molecules varied between 20% and 97%. The methyl radical concentration was found to be in the range 10^{12}–10^{13} molecules cm^{-3}. It was established by analysing the temporal development of the molecular concentrations under static conditions that HCN and NH_3 are the final products of plasma chemical conversion. The fragmentation rates of methane and methanol and the respective conversion rates to methane, hydrogen cyanide and ammonia were determined for different relative proportions of hydrogen to nitrogen.

The novel experimental aspect introduced by Hempel *et al* was the installation of multiple pass optics directly within the plasmas reactor to achieve higher sensitivity. Twenty four passes were realized with the White cell arrangement, leading to an optical length inside the reactor of about 36 m [59]. Figure 3(*b*) shows a ray diagram of the alignment within the White cell [60].

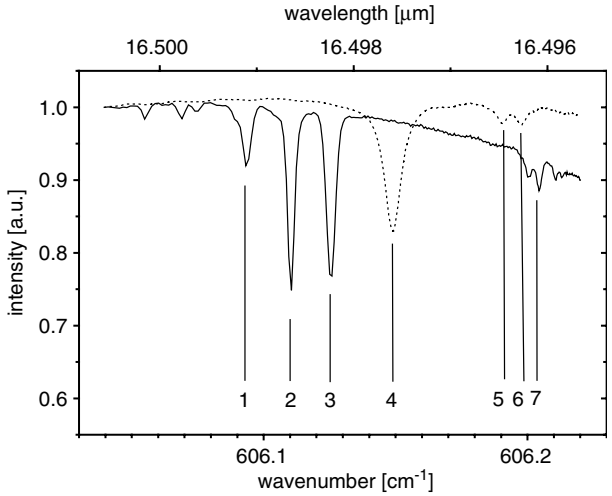

Figure 4. TDL absorption spectra of some methyl and methanol lines in a H_2–Ar–N_2–CH_3OH microwave discharge (1,3,7—CH_3; 2—CH_3OH; 4,5,6—N_2O). The dotted lines due to N_2O are from a reference gas cell placed in the beam path [45].

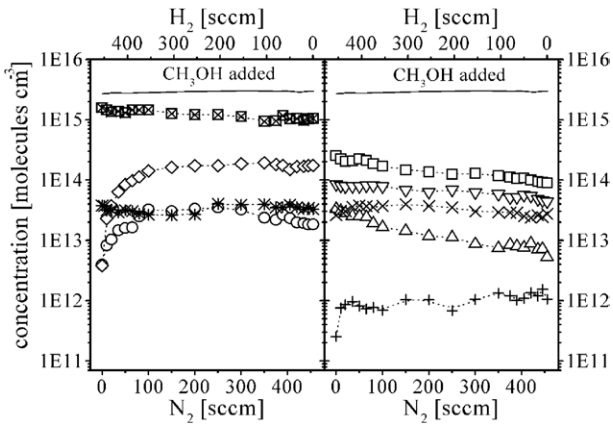

Figure 5. Molecular concentrations in a methanol containing discharge under flowing conditions as a function of the nitrogen/hydrogen flow rate (⊠—T–CH_3OH; ◊—HCN, ○—NH_3, ✳—CH_3, □—CH_4, ×—CH_2O, Δ—C_2H_2, +—C_2H_4, ∇—C_2H_6) [45].

In fact, it is sometimes possible to detect the IR spectra of more than one species in a single laser mode using TDLAS, as shown in figure 4. As an example of the experimental results figure 5 gives an overview of the mass balance and degree of dissociation, as well as the product concentrations which range over five orders of magnitude in a methanol containing discharge under flowing conditions as a function of the nitrogen flow rate. A key objective of this type of study is to be able to model the chemistry of the plasma, for which it is necessary to monitor as many plasma species as possible.

In an earlier paper chemical modelling was successfully used to predict the concentrations of molecular species in methane plasmas in the absence of oxygen and the concentration trends of the major chemical products as oxygen were added [13, 61, 62].

In the work of Hempel *et al* chemical modelling of the methane plasma with admixtures of nitrogen under static conditions was performed to predict the concentrations of those gaseous species which had been detected so far. A total of

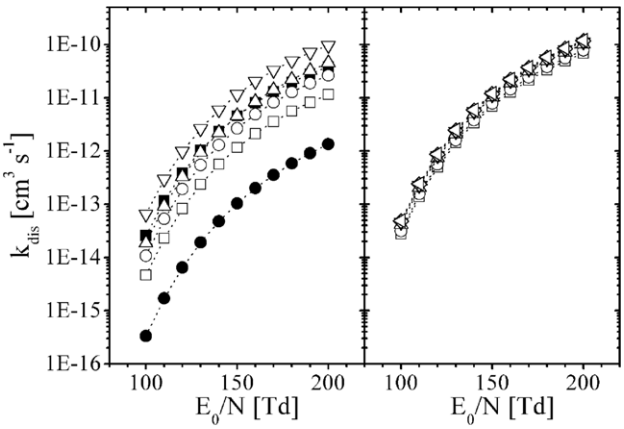

Figure 6. Calculated total electron impact dissociation rate coefficients, k_{dis}, for hydrogen, nitrogen and various hydrocarbons as a function of the reduced electric field strength, E_0/N, (left panel: ■—H_2, ●—N_2, □—CH, ○—CH_2, Δ—CH_3, ∇—CH_4; right panel: □—C_2H, ○—C_2H_2, Δ—C_2H_3, ∇—C_2H_4, ◊—C_2H_5, Ξ—C_2H_6) [45].

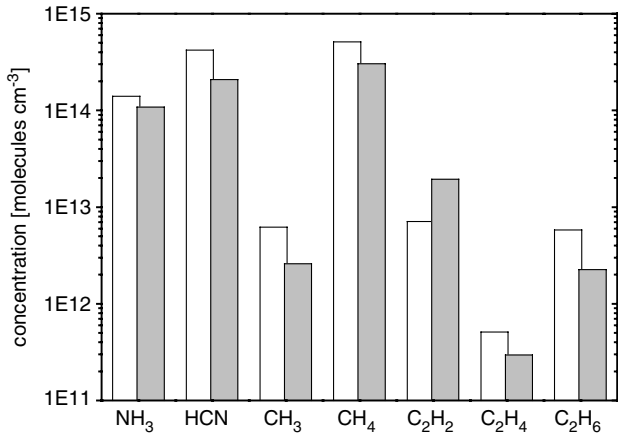

Figure 7. Comparison of species concentrations in a representative H_2–N_2–Ar–CH_4-plasma (white—measured by TDLAS, grey—calculated) [45].

145 reactions for 22 gaseous species were included in the model leading to relatively close agreement of experimental and calculated concentrations and to improved knowledge of the main chemical reaction pathways and plasma chemical processes [45].

The rate coefficients for the electron collision processes have been determined by solving the time-dependent Boltzmann equation for the given values of the reduced electric field, microwave frequency and mixture composition up to the establishment of the steady state. This electron kinetic equation has been solved by means of the multiterm method described by Loffhagen and Winkler [63]. Respective cross sections for electron impact collisions for hydrogen, argon, oxygen and methane were taken from the established literature [61, 64, 65]. Figure 6 shows the calculated total electron impact dissociation rate coefficients for hydrogen, nitrogen and various hydrocarbons as a function of the reduced electric field strength.

A comparison of modelled and experimental species concentrations in a representative H_2–N_2–Ar–CH_4-plasma is presented in figure 7 showing good agreement between them.

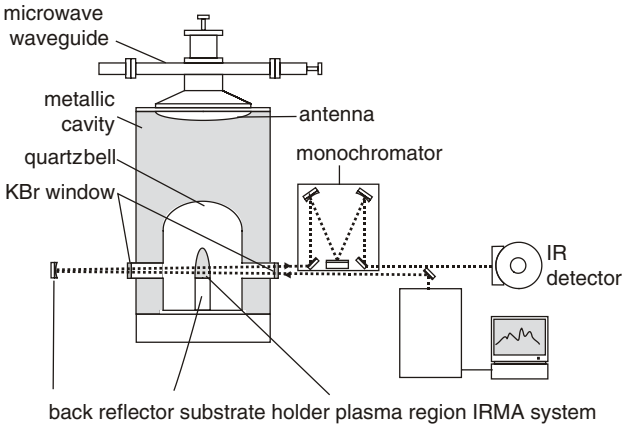

Figure 8. Schematic diagram of the microwave PECVD bell jar reactor used for nanocrystalline and polycrystalline diamond deposition and the integrated TDL spectrometer (IRMA) [68].

2.2.2. Studies in bell jar microwave reactors. Microwave PECVD bell jar reactors are used to produce diamond films with different morphologies depending on the gas mixture used, e.g. poly-crystalline diamond (PCD) for CH_4 strongly diluted in H_2 and nano-crystalline diamond (NCD) for $Ar/H_2/CH_4$ plasmas. The microwave plasmas generated in a bell jar reactor present a very complex chemistry, due to significant thermal gradients between the plasma bulk and the growing diamond surface. In order to improve the deposition process and optimize growth rates, a detailed spatially resolved physico-chemical modelling of the discharge is required. These models need to be experimentally validated, and TDLAS is a particularly relevant tool to provide hydrocarbon densities which can be compared with calculated values.

As an example, one can give a brief comment about studies performed in discharges used for NCD synthesis. Since the demonstration of the feasibility of its deposition ten years ago [66], NCD films have been the subject of increasing interest. This interest was motivated by the fact that, in addition to some physical properties similar to those of PCD, NCD possesses a very low thickness-independent roughness suitable for some tribological and electronic applications that often require very smooth films [66, 67].

In a recent paper Lombardi and co-workers characterized $Ar/H_2/CH_4$ microwave discharges used for nanocrystalline diamond deposition in a bell jar cavity reactor by both experimental and modelling investigations [68]. Figure 8 shows a schematic diagram of the microwave PECVD bell jar reactor used for nanocrystalline diamond deposition and $Ar/H_2/CH_4$ microwave discharge diagnostics. The usual feed gas used for the microwave PECVD process employed for NCD film synthesis is an $Ar/H_2/CH_4$ gas mixture characterized by low H_2 and CH_4concentrations [66].

Discharges containing 1% CH_4 and H_2 percentages ranging between 2% and 7% were analysed as a function of the input microwave power under a pressure of 200 mbar. TDLAS was employed in order to measure the mole fractions of carbon-containing species such as CH_4, C_2H_2 and C_2H_6 present. A thermo-chemical model was developed and used in order to estimate the discharge composition, the gas temperature and the average electron energy assuming a quasi-homogeneous

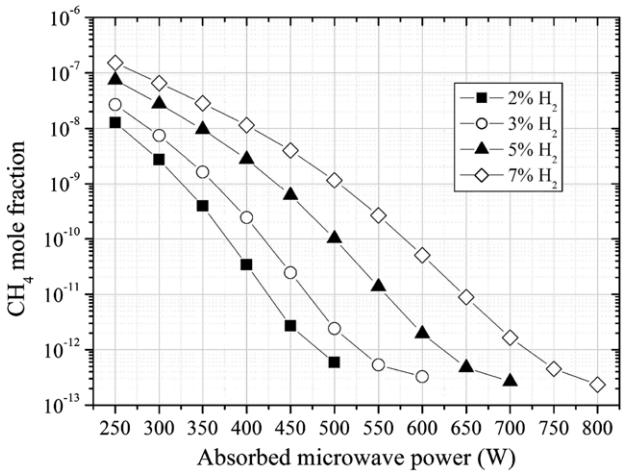

Figure 9. CH_4 mole fraction calculated in the $Ar/H_2/CH_4$ microwave discharges under 200 mbar as a function of the absorbed MWP and for different $\%H_2$ [68].

plasma. Experiments and calculations yielded consistent results with respect to plasma temperature and composition. The CH_4 mole fraction calculated in the $Ar/H_2/CH_4$ microwave discharges under 200 mbar pressure as a function of the absorbed MWP and for different $\%H_2$ is shown in figure 9.

Similar analysis associating modelling and TDLAS measurements were also performed in the case of PCD deposition using H_2/CH_4 plasmas [69, 70], with special emphasis on the detection of the methyl radical which plays a major role in the gas phase chemistry and the deposition process.

2.2.3. Studies in surface wave discharges. A challenging subject of plasma technology is the effective conversion of natural gas, which has methane as the main constituent, to higher hydrocarbons. In the last decade, a variety of papers have been published studying the conversion of hydrocarbons by different experimental and theoretical approaches. Only some recent examples shall be given here; a more comprehensive discussion can be found in [13, 61]. Bugaev *et al* investigated the oxidative conversion of a mixture of natural gas and oxygen in a barrier-discharge by monitoring stable reaction products using gas chromatography [71]. Hsieh *et al* used a RF plasma to convert methane into acetylene, ethylene and ethane, which were detected by Fourier transform infrared spectrometry [72].

In contrast to the many studies of RF plasmas systematic investigations of plasma chemistry and kinetics in molecular surface wave discharges are rather rare. Due to the working conditions of the surface wave discharge, the gas flow and the pressure can be varied over a relatively wide range. Spatial effects appear mainly only in one dimension, in the direction of the discharge tube axis, and can be modelled relatively easily.

TDLAS has been used to detect the methyl radical and four stable molecules, CH_4, C_2H_2, C_2H_4, C_2H_6, in a H_2surface wave discharge (f = 2.45 GHz, power density ≈10–50 W cm^{-3}) containing up to 10% of methane under different flows (Φ : 22–385 sccm) and pressures (p : 0.1–4 Torr). Figure 10 shows the schematic diagram of the experimental set-up [62]. For the TDLAS measurements a compact and

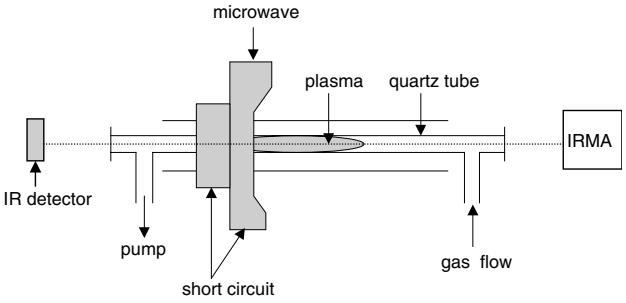

Figure 10. Schematic diagram of the experimental set-up used for studies in surface wave discharges [62].

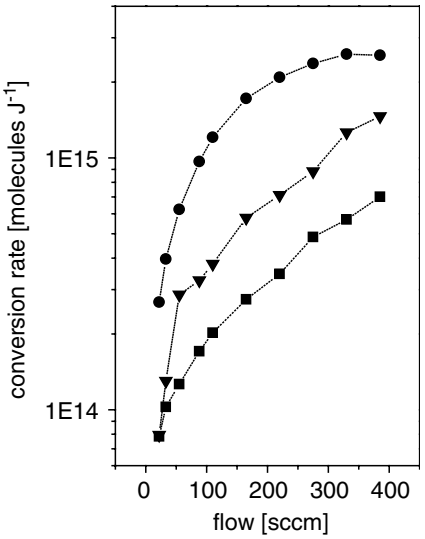

Figure 11. Rate of conversion as a function of flow rate in a H_2–CH_4 plasma from a surface wave discharge measured by TDLAS ($P = 600$ W, $p = 1.3$ mbar, 10% CH_4), ●, C_2H_2; ▼, C_2H_4; ■, C_2H_6 [62].

transportable infrared multi-component acquisition (IRMA) system was used [24].

The degree of dissociation of the methane precursor varied between 20 and 85% and the methyl radical concentration was found to be of the order of 10^{12} molecules cm^{-3}. The methyl radical concentration and the concentrations of the stable C-2 hydrocarbons C_2H_2, C_2H_4, C_2H_6, produced in the plasma, increased with increasing amounts of added CH_4 as well as with increasing pressure. For the first time, fragmentation rates of methane ($R_F(CH_4)$: 1×10^{15}–2.5×10^{16} molecules J^{-1}) and conversion rates to the measured C-2 hydrocarbons ($R_C(C_2H_y)$: 5×10^{13}–3×10^{15} molecules J^{-1}) and their dependence on flow and pressure in a surface wave discharge could be estimated. Figure 11 shows the rate of conversion as a function of flow in a H_2–CH_4 plasma in a surface wave discharge measured by TDLAS. The influence of diffusion and convection on the spatial distribution of the hydrocarbon concentration in the discharge tube was considered using a simple model [62].

The following plasma chemical phenomena were found under flow and pressure variation: (i) a lower degree of dissociation of CH_4 at higher flows but increasing absolute rates of fragmentation leading only to slightly reduced concentrations of the measured C-2 hydrocarbons and (ii) an increasing degree of dissociation with pressure corresponding to higher rates of fragmentation [62].

2.3. Fragmentation of hexamethyldisiloxane in RF discharges

Plasmas containing organosilicon precursors are used in a variety of plasma enhanced chemical vapour deposition (PECVD) processes to deposit thin films with advantageous mechanical, electrical or optical properties. For many years the well-established plasma-assisted polymerization technique has been based on hexamethyldisiloxane (HMDSO), $(CH_3)_3$–Si–O–Si–$(CH_3)_3$, one of the simplest siloxane compounds [73]. Nevertheless, to open up new applications the deposition of coatings with a wide range of chemical and physical properties by varying plasma parameters is a challenging topic in plasma technology.

The analysis of the properties of various discharges containing HMDSO and of the chemical structure of deposited layers has a long and interesting history; for details see [74,75]. As far as it is known, no absolute concentrations of reaction products in HMDSO plasmas have been ever measured. Only in his early paper in 1973 Schmidt used mass spectrometry to determine the fraction of reaction products in HMDSO glow discharges under static conditions [76]. In 1994 based on mass spectrometry, the same group published estimates of the relative concentrations of methyl and methane in HMDSO/Ar discharges [77].

Recently spectroscopic diagnostic studies of pure HMDSO plasmas and of admixtures of argon in a low-pressure, asymmetric, capacitively coupled radio frequency discharge ($f = 13.56$ MHz) have been described [75]. In these TDLAS studies, the methyl radical and three stable molecules, CH_4, C_2H_2 and C_2H_6, were detected. For the first time the methyl radical concentration and the concentration of hydrocarbons, produced in the plasma, have been measured while the discharge power ($P = 20$–200 W), total gas pressure ($p = 0.08$–0.6 mbar) and gas flow rate ($M = 1$–10 sccm) were varied. One of the objectives was to determine conversion rates into the measured hydrocarbons as a function of flow, power and pressure. The analysis of gas phase phenomena was completed by deposition experiments and by mass spectrometric studies.

The experimental arrangement of the low pressure, asymmetric RF discharge and the tuneable diode laser (TDL) system is shown in figure 12. As an example, figure 13 presents molecular concentrations as a function of power in a pure HMDSO plasma measured by TDLAS. This figure gives an overview of the mass balance and of hydrocarbon product concentrations, ranging over three orders of magnitude, in pure HMDSO plasmas. An increasing amount of power coupled to the plasma leads to higher concentrations of the (measured) stable hydrocarbons reaching saturation values at about 80 W [75].

The methyl radical concentration was found to be of the order of 10^{13} molecules cm^{-3}, while methane and ethane were the dominant stable hydrocarbons with concentrations of 10^{14}–10^{15} molecules cm^{-3}. Conversion rates to the measured stable hydrocarbons ($R_C(C_xH_y)$: 2×10^{12}–2×10^{16} molecules J^{-1} s^{-1}) could be estimated as a function of power, flow, mixture and pressure. Under the experimental conditions used, a maximum polymer deposition rate of about 400 nm min^{-1} was found [75].

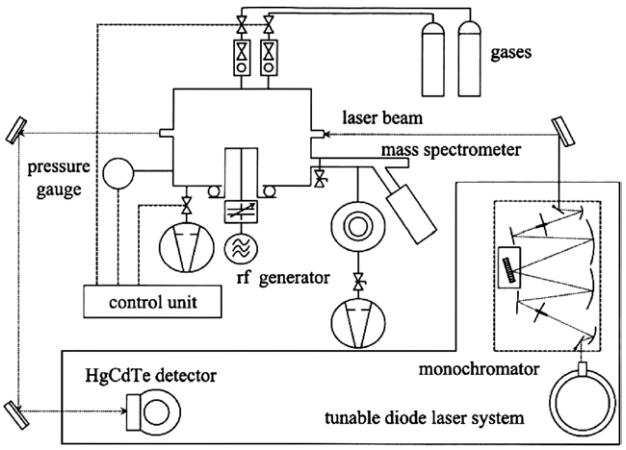

Figure 12. Experimental set-up for studies of fragmentation of hexamethyldisiloxane in RF discharges [75].

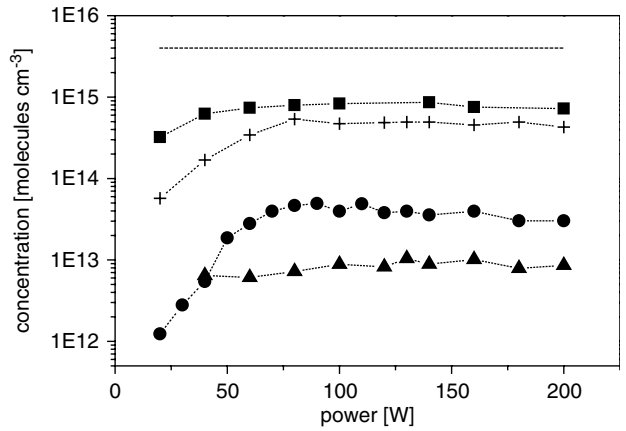

Figure 13. Molecular concentrations as a function of power in a pure HMDSO plasma measured by TDLAS ($\Phi_{HMDSO} = 5$ sccm, $p = 0.15$ mbar), dashed line: added HMDSO; ■, C_2H_6; +, CH_4; ●, C_2H_2; ▲, CH_3 [75].

2.4. On NO_x production and volatile organic compound removal

Recent concerns about air quality have led to increasing research in the field of pollution abatement from gas exhausts. Apart from conventional techniques, such as catalysis, scrubbers and active carbon, the use of electric discharges is a promising technique for toxic gas removal, especially when these gases are present in low concentrations [78–83]. There is of course a wealth of literature dealing with the NO_x problem and so only a single example dealing with new aspects is presented here.

One of the key issues when studying plasma processing for gas treatment is to make sure that no undesirable by-product results from the process. Among them, NO_x compounds are readily produced in air plasmas. The production of undesirable NO and NO_2 and the removal of 3-pentanone, an example of a volatile organic compound (VOC), has been studied in a pulsed microwave discharge in air at near atmospheric pressures. The influence of changing pulse duration from 25 to 500 μs and of the pulse repetition rate from 10 to 500 Hz is reported. At a relatively high pressure of $p = 800$ mbar plasma ignition

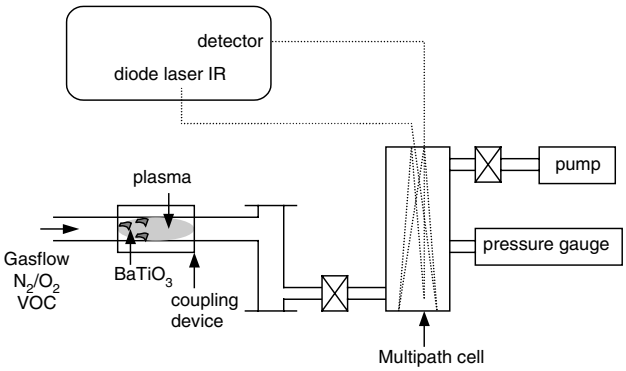

Figure 14. Experimental set-up: plasma generator, laser device and the multipass cell where the infrared laser beam is collimated. The microwave power is injected into the plasma via a 'surfaguide'. The plasma is generated in a quartz tube in contact with high dielectric permittivity $BaTiO_3$ pellets. The gas pressure is 800 mbar in the plasma reactor and 1 mbar in the multipass cell [84].

is achieved by inserting $BaTiO_3$ pellets inside the microwave excitator.

Both NO and NO_2 could be measured simultaneously using TDLAS spectroscopy in the infrared region. NO_x densities as high as several thousands ppm were found to be produced at high specific energies. In contrast to what was expected, the use of short pulses did not lead to an effective curtailment of the NO_x production. It was found that the NO_x formation depended only on the average power injected into the plasma independent of the pulse duration and repetition rate.

Furthermore, the efficiency of the pulsed microwave discharge for VOC oxidation, in this case of 1400 ppm of 3-pentanone in dry air, has been studied. The VOC removal efficiency was determined using gas chromatography. The oxidative efficiency of the discharge was found to increase linearly with the pulse repetition rate as well as with the pulse duration, the power duty cycle ratio being the key parameter [84]. Figure 14 shows the experimental set-up: plasma generator, laser device and the multipass cell where the infrared laser beam is collimated. In figure 15 the production of NO and NO_2 as a function of the pulse duration for different pulse repetition rates is shown.

2.5. Detecting boron hydrides in microwave plasmas

Non-equilibrium low-pressure plasmas containing boron, commonly used in combination with other reactive molecular gases, are widely employed for surface treatment in a variety of PECVD processes, for example, to deposit thin hard films of diamond or boron nitride [85–90]. Also this type of plasma is used for producing semiconductors and thermo-polymers and is also of interest in astrophysics and for jet engines and rocket propulsion. Various precursor molecules such as BCl_3, BF_3 or B_2H_6 are used to provide boron containing species in the plasma.

In contrast to the rather widespread application of plasmas containing boron and hydrogen not much is known about internal plasma properties and phenomena, including processes of precursor fragmentation, plasma heating and related dissociation processes.

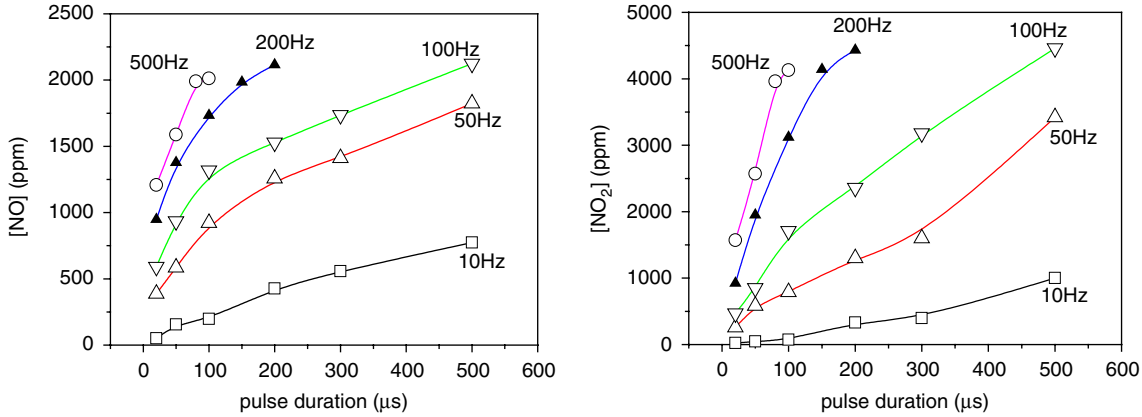

Figure 15. Production of NO and NO_2 as a function of the pulse duration for different pulse repetition rates. The gas flow rate was 250 sccm of dry air ($N_2 : O_2 = 4 : 1$) at 800 mbar [84].

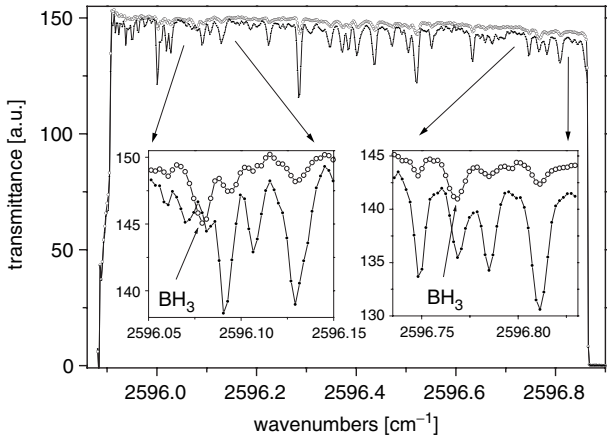

Figure 16. Part of the absorption spectrum of diborane recorded in the H_2–Ar–B_2H_6 (64 : 33 : 3) gas flow (dots) and in the H_2–Ar–B_2H_6 discharge plasma at $p = 1.5$ mbar, $P = 1.5$ kW (open circles). The arrows show two spectral lines of the Q branch of the BH_3 radical produced in the plasma, at 2596.077 cm^{-1} $Q(3, 0)$ and 2596.764 cm^{-1} $Q(1, 0)$ [94].

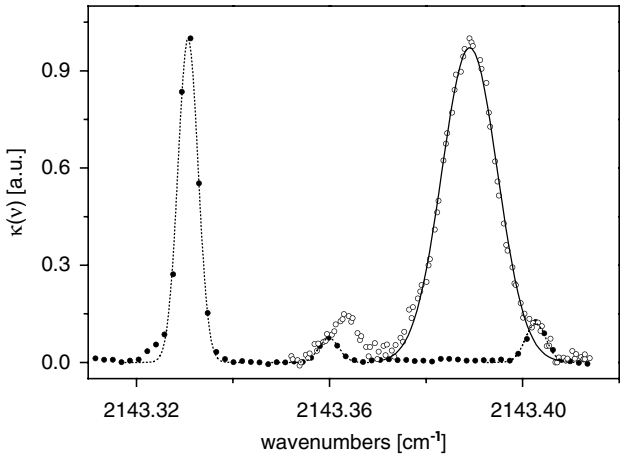

Figure 17. The spectral distribution of the absorption coefficient of N_2O (●) and BH (○) molecules measured in a N_2O reference gas cell and in a H_2–Ar–B_2H_6 microwave plasma ($P = 2.5$ kW, $p = 2.5$ mbar). The proportions in the H_2–Ar–B_2H_6 gas mixture were (64 : 33 : 3) [94].

The structure and molecular constants of the BH_3 molecule were determined from the analysis of its ν_2 and ν_3 fundamental bands by TDLAS and FTIR, respectively [91,92]. Chemical aspects of boron nitride deposition in Ar–B_2H_6–NH_3 and Ar–B_2H_6–N_2 RF discharges were studied by FTIR absorption spectroscopy [87]. In the spectral range between 500 and 3500 cm^{-1} several diborane bands were detected. It was observed that their intensity decreased due to B_2H_6 dissociation caused by the discharge activity.

The basic spectroscopy and reaction kinetics of diborane and its fragmentation products, BH_3 and BH [93], have been widely studied, but investigations of the behaviour of these boron hydrides in non-equilibrium plasmas are uncommon. Only in their recent FTIR study of Ar–B_2H_6–NH_3 and Ar–B_2H_6–N_2 RF discharges did Franz *et al* find, not surprisingly, a decreased absorption of diborane bands in the plasma compared with the gas phase. They were able to roughly estimate the degree of dissociation of the precursor but the behaviour of the other fragmentation products was not reported [87].

The TDLAS measurements were performed with the IRMA system to measure absorption lines of B_2H_6, BH_3 and BH. For the detection of the BH radical an optical multiple pass arrangement was used providing higher sensitivity.

Since the TDLAS method does not provide overview spectra over a wide range selected spectral windows were chosen, where absorption features of the species of interest such as B_2H_6, BH_3 and BH could be expected. An example of absorption spectra containing lines of B_2H_6 and BH_3 is presented in figure 16. Although the infrared spectrum of B_2H_6 is rather rich in lines in the vicinity of 2596 cm^{-1}, two BH_3 lines, even at absorptions less than a few per cent, can be clearly identified.

The analysis of the profile of two BH absorption lines of the 1–0 band of the BH $X^1\Sigma^+$ state, at 2143.39 cm^{-1} and at 2170.0391 cm^{-1} [94], provided an additional approach to measure the gas temperature (figure 17). A typical example of an absorption spectrum of BH together with N_2O lines used for identification and calibration of the wavenumber is shown in figure 17.

Normalized on the maximum, or in the case of diborane normalized on its absorption with the plasma off, the absorption coefficients of B_2H_6, BH_3 and BH lines as a

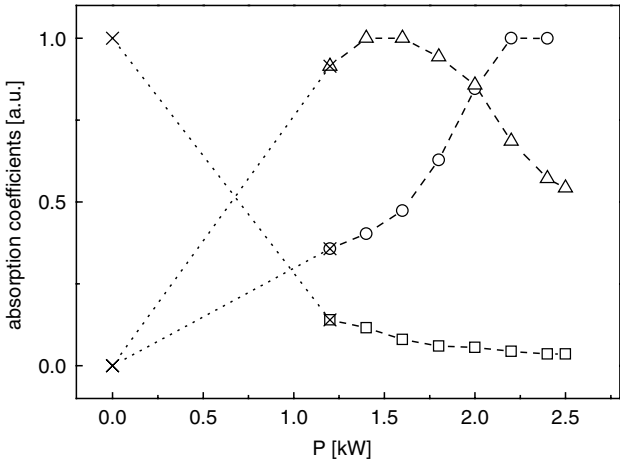

Figure 18. Integral absorption coefficients of B_2H_6 (□—line at position 2596.280 cm^{-1}), BH_3 (Δ—line at 2596.077 cm^{-1}) and BH (○—line at 2143.39 cm^{-1}) measured in the H_2-Ar-B_2H_6 discharge plasma (64 : 33 : 3 a gas mixture) as a function of the microwave power ($p = 1.5$ mbar, $\Phi = 150$ sccm, in the case of diborane normalized on its absorption in the gas flow without discharge). For clarity, straight lines are drawn from $P = 1.4$ kW to $P = 0$ kW [94].

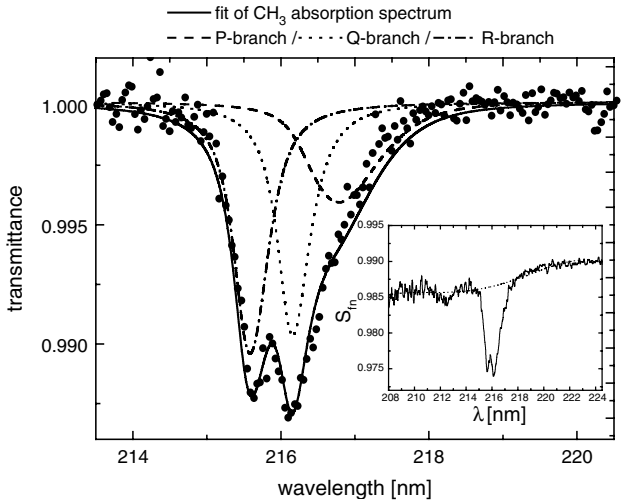

Figure 19. Ultraviolet transmission spectrum of methyl in a H_2–CH_4 microwave plasma in the bell jar reactor. The measured spectrum is fitted by a calculated spectrum representing a sum of the P-, Q- and R-branches of the $B(^2A_1') \leftarrow X(^2A_2'')$ transition. A polynomial fit, shown inset, was used to determine the baseline. ($p = 25$ mbar, $P = 600$ W, MWPD $= 9$ W cm^{-3}, $\Phi_{total} = 200$ sccm, $H_2 + 4\%$ CH_4 admixture [35]).

function of the discharge power are shown in figure 18. The increase in electron density (due to the increase in microwave power) leads to a decrease in the density of diborane in favour of BH_3 up to a maximum around $P = 1.6$ kW. On further increasing the power the BH_3 density decreases while the diatomic molecule boron hydride (BH) shows a rapid growth in its density. This behaviour should be considered as direct evidence of the electron impact character of the dissociation in the present conditions. The straight dotted lines drawn in figure 18 from 0 to 1.4 kW represent possible trends of the population densities of those species in the plasma. Unfortunately, absolute values of the particle densities cannot be obtained yet because of the lack of assignment of the absorption lines to certain rovibronic transitions (in the case of B_2H_6) and of values of the corresponding Einstein coefficients for the boron hydrides under study. The determination of line strengths of the transient molecules, BH_3 and BH, would be of great importance for further quantifying measurements (for details see [94]).

3. Kinetic studies and molecular spectroscopy of radicals

3.1. Comparative study of CH_3 detection by IR-TDLAS and UV absorption techniques

The methyl radical is important not only in carbon film deposition plasmas but also in combustion and in atmospheric and interstellar molecular chemistry. Although in recent years several studies to quantify the methyl concentration in hydrocarbon plasmas have been performed in the ultraviolet and infrared spectral range, never have both spectroscopic approaches been compared directly to verify the applicability of the absorption cross sections or line strengths for the conditions under study. This comparison is of particular importance since the validity of the line parameters is directly related to the accuracy of calculated methyl concentrations and in turn to the quality of related plasma chemical modelling.

For the purpose of concentration measurements, the frequencies, absorption cross sections or line strengths and the pressure broadening coefficients of the lines need to be known accurately. Unfortunately, the number of quantitative studies is relatively small and the validity of the reported values is limited (for details see [35]).

Recently a comparative study has been performed in plasmas of two different microwave reactors ($f = 2.45$ GHz), (i) in H_2–Ar plasmas with small admixtures of methane or methanol in a planar microwave reactor, at a pressure of 1.5 mbar, and (ii) in H_2–CH_4 plasmas in a bell jar reactor, at pressures of 25 and 32 mbar.

The planar microwave plasma reactor used for these experiments is comparable to that shown in figure 3(*a*). Details of the reactor, the infrared tuneable diode laser and broadband ultraviolet spectrometer can be found elsewhere [95–97]. A schematic diagram of the bell jar reactor together with the optical arrangement is shown in figure 8 [33, 35, 98].

For classical absorption measurements in the ultraviolet spectral range a deuterium lamp is the light source and a monochromator of medium spectral resolution combined with (i) an optical multi-channel analyser as detector (method 1) or (ii) employing chopper modulation and a photo multiplier detector together with a lock-in amplifier (method 2). In the current work, the absorbance of the methyl radical in the ultraviolet spectral region was determined by the best fit of the measured spectrum to a calculated spectrum representing the P-, Q- and R-branches of the $B(^2A_1') \leftarrow X(^2A_2'')$ transition. Figure 19 shows a typical example of an ultraviolet transmission spectrum of methyl, together with the related fits, in a H_2–Ar–CH_3OH microwave plasma using the planar reactor.

For infrared absorption measurements in the planar reactor, a one-channel TDLAS system [13] and, in the bell jar reactor, the IRMA system were used [24]. The data acquisition method was an advanced form of sweep integration including

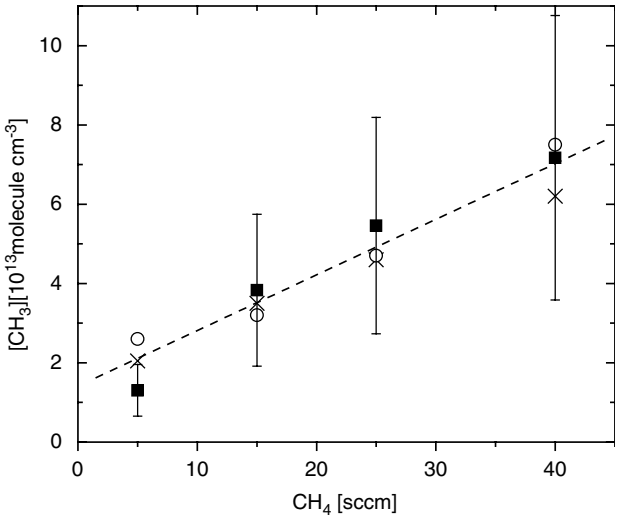

Figure 20. The concentration of the methyl radical as a function of the methane admixture in the planar microwave reactor measured by ultraviolet and infrared absorption techniques (■—TDLAS $Q(3,3)$ line, ×—UV absorption method 1, ○—UV absorption method 2, $p = 1.5$ mbar, $P = 1.5$ kW, $\Phi_{\text{total}} = 555$ sccm) [35, 101].

the non-linear least-squares fitting of the methyl line shapes [99, 100].

Figure 20 shows the concentration of the methyl radical as a function of the flow rate of methane measured by ultraviolet and infrared absorption techniques in the planar microwave reactor. Taking into account the uncertainties of the UV absorption cross section and of the line strength, the data shown in figure 20 demonstrate that the results of both techniques are in excellent accord. In addition to data former published by Lombardi *et al* [35] the influence of stimulated emission has been considered [101]. In summary, the present comparative quantitative study of the methyl radical by broadband ultraviolet and infrared absorption techniques in the non-equilibrium plasma of a planar microwave reactor has led to a significant result: the application of the CH_3 absorption cross section of the $B(^2A_1') \leftarrow X(^2A_2'')$ transition at 216 nm, reported by Davidson *et al* [96], and of the line strength of the $Q(8,8)$ line of the ν_2 fundamental band near to 16.6 μm, found by Wormhoudt and Mc Curdy [37], gives, within the errors of the measurements and of the spectroscopic data, the same concentration. For further details see Lombardi *et al* [35].

3.2. Line strengths and transition dipole moment of CH_3

This section describes a new measurement of μ_2 for the ν_2 fundamental band of the methyl radical in order to resolve the differences between earlier experimentally measured values and between experiment and theory. The method used for determining the absolute methyl radical concentrations was the same as that used by Yamada and Hirota [15]. However, integrated intensities and many more methyl radical lines were used. Furthermore, the kinetic conditions were more precisely specified and the temperature determined more exactly. The resulting value of μ_2 is now in much better agreement with theory.

The methyl radical has no electric dipole allowed rotational transitions because of its D_{3h} symmetry and so

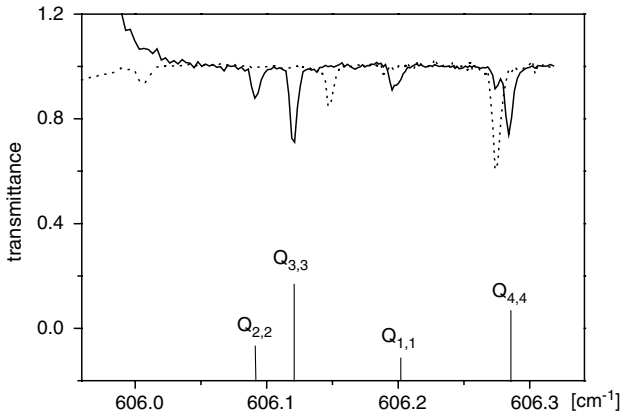

Figure 21. Survey spectrum showing several ($J = K$) Q branch lines of the ν_2 fundamental of the CH_3 free radical around the band origin. The spectrum represented by the dashed line is a calibration spectrum from N_2O and CO_2 [38].

IR spectroscopy is one of the few suitable methods for its detection. The determination of methyl radical concentrations in terrestrial and astronomical sources using IR spectroscopy relies on the availability of accurate line strengths and transition dipole moments. The ν_2 band of CH_3 is the strongest among its IR active fundamentals and particularly useful for quantitative measurements. The need for a more accurate and precise value of μ_2 has been highlighted by the measurements of CH_3 in the atmospheres of Saturn [102], Neptune [103] and in the interstellar medium [104].

The experimental set-up of the planar microwave plasma reactor with the optical arrangements used for the methyl transition dipole moment study is comparable to that shown in figure 3(*a*). Details of the diode laser spectrometer, IRMA, and discharge absorption cell have been reported elsewhere [24, 46]. The methyl radical was produced in mixtures of tertiary butyl peroxide ($[(CH_3)_3CO]_2$) and argon at a total pressure of 1 mbar. Two kinds of experiment were performed: (a) time-dependent measurement of the decay of the absorption coefficient when the discharge was turned off, to obtain absolute methyl concentrations and (b) measurements of the absorption coefficients of different rovibronic lines. In total ten lines were studied in the fundamental band, seven in the first hot band and one from the second hot band. A survey spectrum of the Q-branch region of the ν_2 fundamental band is shown in figure 21.

In order to derive accurate line strengths and the transition dipole moment, it is necessary to obtain the absolute concentration of the methyl radical and its temperature in the discharge. The decay method was the experimental approach for methyl radical concentration measurements. The plasma was switched on and off for periods of ten seconds and the decay of the methyl radical signal measured during the off period with ms time resolution [99, 100]. The absolute concentration was obtained from the decay of the integrated absorption coefficient and the recombination rate constant. It is well known from numerous kinetic studies that the main loss channel under the conditions used here is self-recombination via a three body reaction. Hence, by measuring the integrated absorption coefficient as a function of time and knowing

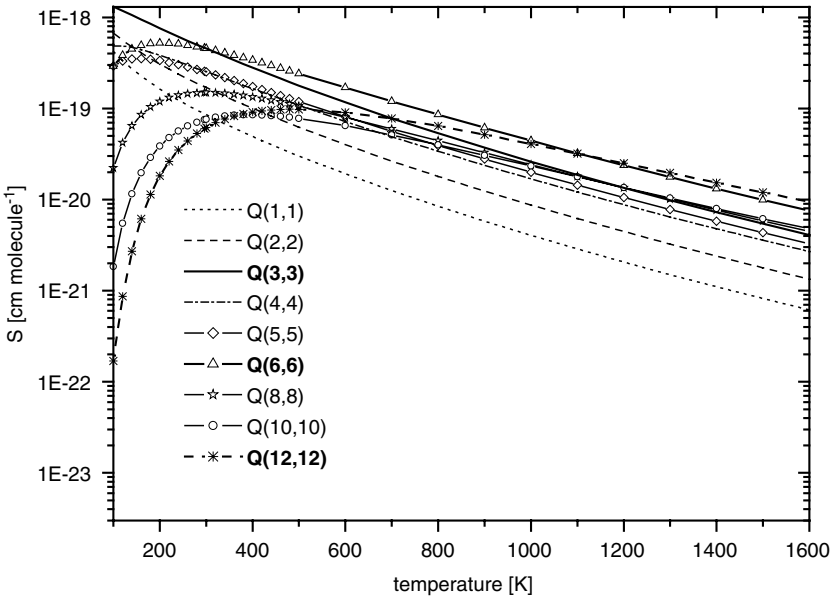

Figure 22. Line strengths, S, for different Q branch transitions of CH_3 as a function of temperature. Values calculated from the reference temperature values at 296 K [38].

the value of the recombination rate constant the absolute concentration of the methyl radical can be obtained.

The rate constant k_1 for the self-recombination reaction of methyl radicals has been extensively investigated in experimental and theoretical work [105–112]. The selected value for k_1 was based on the compilation of Baulch *et al* and was appropriate for the specific temperature and argon concentration [38, 113]. The translational, rotational and vibrational temperatures of the methyl radical were measured. A near similarity of T_{trans} and T_{rot} was observed. Based on experimental results the vibrational temperature was found to be in equilibrium with the translational and rotational temperature within experimental uncertainties, i.e. $T_{vib} = 600$ K. For details see [38, 101].

Figure 22 shows an example of the temperature dependence of the line strengths of several transitions from the lower energy levels. The line strengths have been calculated from the experimental data. It should be mentioned that the line strength dependences can be used to determine the gas temperature when two absorption coefficients are measured. Measuring the ratio of two absorption coefficients is the same as the ratio of their line strengths. Taking a measured absorption coefficient ratio, the temperature for which their line strength ratio is the same determines the rotational temperature. In recent measurements (not shown here) which were done in a hot filament diamond deposition reactor [114] the gas temperature has been determined from the ratio of $Q(6, 6)$ and $Q(12, 12)$. The gas temperature was found to be about 800 K near the deposition substrate, which was essentially the same as the temperature measured by a thermocouple probe.

The line strengths of the nine Q branch lines in the ν_2 fundamental band of the methyl radical in its ground electronic state were used to derive a more accurate value of the transition dipole moment of this band: $\mu_2 = 0.215(25)$ Debye. Improved accuracy over earlier measurements of μ was obtained by integrating over the complete line profile instead of measuring the peak absorption and assuming a Doppler line width to deduce the concentration and the derivation of more accurate temperatures by examining a large number of lines. In addition a more precise value for the rate constant for methyl radical recombination than available earlier was employed. The new value of μ_2 is in very good agreement with high quality *ab initio* calculations. Furthermore, the ratio of the transition dipole moments of the ν_2 and ν_3 fundamental bands in the gas phase is now in highly satisfactory agreement with the ratio determined for the condensed phase. Figure 23 shows the chronological summary of calculated and measured values of μ_2 the transition dipole moment of the ν_2 fundamental band.

3.3. Molecular spectroscopy of the BO radical

Transient molecular species, to be found in the gas phase and in plasmas in particular free radicals, are amongst the most fascinating species in the field of molecular spectroscopy. They are of special importance for several areas of reaction kinetics and chemistry. The study of the high resolution spectra of radicals provides a very effective approach to understand their properties and dynamics. There is continuing interest in the boron and oxygen containing intermediates [115] that may be formed during the oxidation of elemental boron leading eventually to the final, thermodynamically stable, oxide product, B_2O_3. However, relatively little is known about the spectroscopy of these species in the gas phase. Only the simple oxides BO and BO_2 have been investigated in detail by high-resolution spectroscopy. Both of these radicals have electronic emission spectra in the visible region of the spectrum. In the case of BO there are two extensive band systems, the $A^2\Pi$–$X^2\Sigma$ and $B^2\Sigma$–$X^2\Sigma$, which have been studied since the early days of quantum mechanics, for example, by Mulliken [116]. Most relevant are the recent analyses of these band systems by Coxon *et al* [117] and Mélen *et al* [118]. In addition, the microwave spectra of the two lowest rotational transitions of the radical have been reported by Tanimoto *et al* [119].

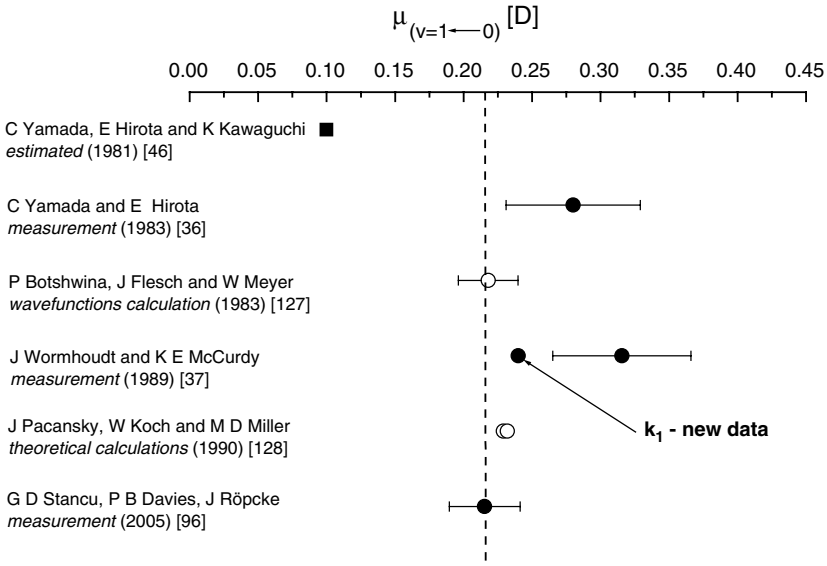

Figure 23. Chronological summary of calculated and measured values of μ_2, the transition dipole moment of the ν_2 fundamental band of CH_3 [38].

Recently, a study has reported on the fundamental bands of the ^{10}B and ^{11}B isotopomers of BO in their ground $^2\Sigma^+$ states, detected in natural abundance in the O + BCl_3 reaction, at Doppler limited resolution using tuneable diode laser absorption spectroscopy. It extended a preliminary study reported earlier, in which only the spectrum of ^{11}BO was examined quantitatively [120]. The radicals were made in a 1 m long White-type absorption cell with 26 passes, following the method described by Clyne *et al* and Llewellyn *et al* [121,122]. Oxygen atoms were produced by partially titrating a flow of nitrogen atoms, generated in a 2.45 GHz microwave discharge in molecular nitrogen, with nitric oxide to just below the end point so that some nitrogen atoms remained in the gas flow. Boron trichloride vapour was then added to produce an intense, light blue chemiluminescence from the emission of BO.

The fundamental band origins for $^{10}B^{16}O$ and $^{11}B^{16}O$ are found to be 1915.30674(14) cm^{-1} and 1861.92409(13) cm^{-1}, respectively. The rotational constants for the lower states are 1.877680(22) cm^{-1} and 1.773421(10) cm^{-1}, which are in excellent agreement with the microwave values for B_0. Assuming a linear dependence of B_v on $(v + \frac{1}{2})$ the derived value of R_e is 1.204552(5) Å. The stick diagram shown in figure 24 displays the detected lines for both species calculated at a rotational temperature of 300 K [123].

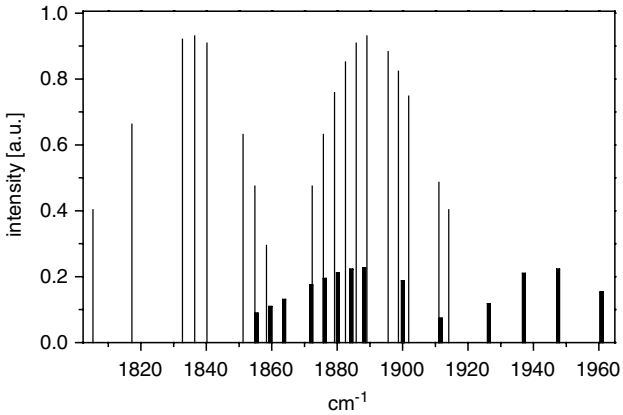

Figure 24. Stick diagram of the measured $^{10}B^{16}O$ (bold) and $^{11}B^{16}O$ lines. The intensities were calculated for 300 K [123].

3.4. Molecular spectroscopy of the CN radical

The CN radical is of fundamental importance in laboratory spectroscopy and in astrophysics. Electronic emission spectra arising from the red ($A^2\Pi$–$X^2\Sigma^+$) and violet ($B^2\Sigma^+$–$X^2\Sigma^+$) band systems excited in flames and discharges have been studied in the laboratory over decades while CN spectra have been detected in the atmospheres of stars and in the interstellar medium. Most recently the electronic band systems have been very extensively measured and analysed in emission [124,125] using high resolution Fourier transform spectroscopy.

Rotationally resolved spectra of the fundamental band of the CN free radical in four isotopic forms have been measured using tuneable diode laser absorption spectroscopy [126]. The source of the radical was a microwave discharge in a mixture of isotopically selected methane and nitrogen diluted with argon. The lines were measured to an accuracy of 5×10^{-4} cm^{-1} and fitted to the formula for the vibration rotation spectrum of a diatomic molecule, including quartic distortion constants. The band origins of each of the isotopomers from the five parameter fits were found to be $^{12}C^{14}N$: 2042.42115(38) cm^{-1}, $^{13}C^{14}N$: 2000.08479(23) cm^{-1}, $^{12}C^{15}N$: 2011.25594(25) cm^{-1}, $^{13}C^{15}N$: 1968.22093(33) cm^{-1} with one standard deviation from the fit given in parenthesis. Some of the lines showed a resolved splitting due to the spin rotation interaction. This was averaged for fitting purposes. The average equilibrium internuclear distance derived from the $v = 0$ and $v = 1$ rotational constants of the four isotopomers is 1.171800(6) Å which is in good agreement with the value determined from microwave spectroscopy. Figure 25 shows a stick diagram of all the lines measured in the four isotopic forms and their intensities calculated for a rotational temperature of 950 K [126].

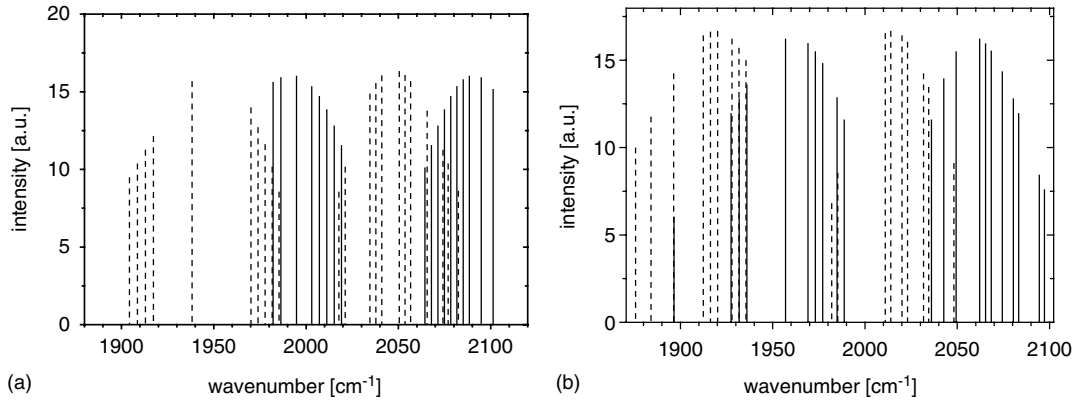

Figure 25. Stick diagrams showing the detected absorption lines from the fundamental band of CN and their intensities at 950 K: (*a*) $^{12}C^{14}N$ and $^{13}C^{14}N$ (· · · · ·) and (*b*) $^{12}C^{15}N$ and $^{13}C^{15}N$ (· · · · ·) [126].

Figure 26. Photograph of the IRMA system: left—optical table, right—data acquisition rack with diode laser controllers and industrial computers [24].

4. Infrared absorption for plasmas diagnostics and control

4.1. The IRMA system

In order to exploit the capabilities of infrared tuneable diode laser absorption spectroscopy for effective and reliable on-line plasma diagnostics and process control in research and industry, a compact and transportable tuneable infrared multi-component acquisition system (IRMA) has been developed [24]. Figure 26 shows a photograph of the complete IRMA system including the optical table and the data acquisition rack.

The IRMA system contains four independent laser stations. The narrowband infrared emission of four lead-salt diode lasers, which can be temporally multiplexed, is used to monitor the infrared absorption features of the target species. The arrangement of the instrument optical table has the dimensions of 110 × 60 cm^2. The four diode lasers are mounted in individual cold stations, which are thermally coupled to the cold finger of a closed cycle cryostat. The temperature of each laser is controlled at milli-Kelvin precision between 30 and 100 K. A single cold station can be heated up to room temperature and decoupled from the main vacuum to allow laser replacement in typically 90 min with the other laser stations remaining operative. Four grating monochromators serve as mode filters. The light of the four lasers is converged into a single beam, which is used for measurement and reference purpose, respectively. The measurement path can either be passed through a measurement cell, for example a plasma, external to the optical table or through an internal multi-path astigmatic Herriot cell. This cell with a path length of 36 m is included for exhaust gas detection. In the reference path, the spectral absorption from small optical cells containing the target gas at high concentration is monitored as input for a laser emission wavelength control loop (line-locking). The two measurement beams and the reference beam are focused on photoconductive infrared detectors mounted in liquid nitrogen cooled dewars.

The data acquisition system for the four-channel tuneable diode system consists of two computers combined with two high speed (300 kHz) boards and two dual diode laser controllers housed in a single transportable rack (figure 26). Based on rapid scan software using direct absorption with sweep integration, the absolute concentrations of several molecular species can be measured simultaneously within milliseconds and used as digital output for on-line process control. The software of the system is able to fit up to four species simultaneously using up to 45 individual spectral lines per species.

The result of time-dependent species density measurement is useful especially for process control. The burst data acquisition mode provides the highest possible time-resolution by transferring fifty measured spectra directly to the extended memory of the computer following a trigger pulse [24]. The IRMA system has been applied successfully in several studies of molecular phenomena in plasmas, e.g. [38, 62, 68, 70, 94, 128, 129].

4.2. The TOBI system

For further progress in understanding molecular processes, in particular in plasmas under non-stationary excitation conditions, there is a need for improved temporal resolution of TDLAS, i.e. for improved, sensitive high speed diagnostics. For these purposes a compact and transportable two laser beam infrared (TOBI) (figure 27) system has been designed for simultaneous measurement of two gaseous species with two tuneable lasers operating simultaneously. In comparison

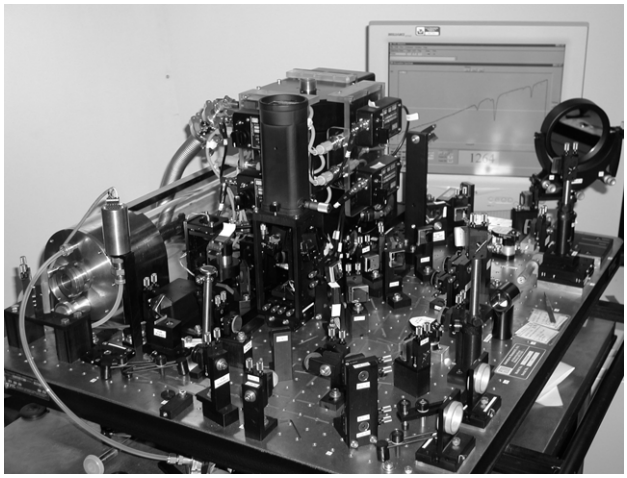

Figure 27. Photographic overview of the TOBI system [25].

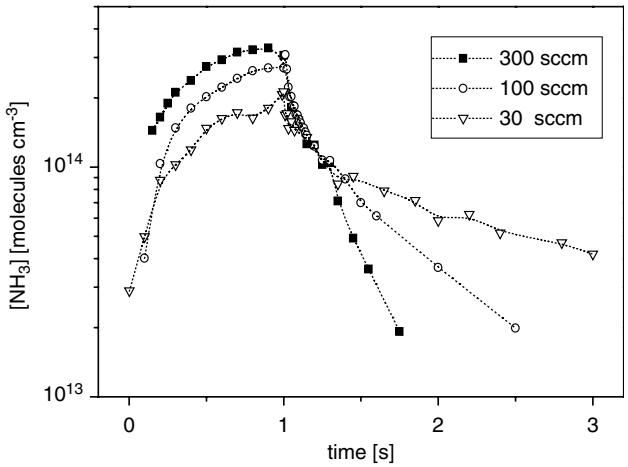

Figure 28. Example of NH_3 concentrations as function of time in a pulsed N_2–H_2 surface wave discharge ($f = 2.45$ GHz, $P_{pulse} = 1$ kW, pulse $= 1$ s, of period $= 5$ s, flow conditions, $N_2/H_2 = 9/1$, $p = 1.3$ mbar) [25].

Figure 29. Q-MACS-Basic system with laser head (left-hand side, size 700 cm^3), supply unit and connection cable [131].

with the IRMA system TOBI is mainly focused on high speed detection. A new generation of rapid scan software for the Windows operating system ('TDL Wintel') allows investigation of transient plasma conditions on time scales of tens of microseconds. This program implements direct absorption with sweep integration to measure the absolute concentrations of several molecular species and provides continuous digital output, which can be used for process control. The TDL Wintel program has many further advanced features. This includes several convenient frequency locking options as well as methods for suppressing background interference. The laser sweep and signal digitization cycle can be synchronized with a pulsed plasma apparatus. The program will collect spectra which are the ratios of the spectra with the discharge on to those with the discharge off. This provides a highly sensitive method for searching for transient species. The software also provides spectral simulation, remote instrument operation and gas concentration calibration.

The optical system can switch between two measurement modes, either directing the probe beams through the plasma apparatus or through a 100 m multi-pass cell to measure gas extracted from an operating plasma. The capabilities of the TOBI system have been demonstrated in plasmas of pulsed H_2–N_2 surface wave and pulsed air–CH_4 DC discharges (figure 28). The potential use of the TOBI system can be summarized as being mainly focused on (i) the high speed detection of transient molecular species, radicals and molecular ions, in plasmas under non-stationary excitation conditions using fast external detectors, and on (ii) the sensitive (sub-ppb) trace gas detection based on the multi-pass absorption cell [25].

4.3. The Q-MACS system

For reasons of enhanced efficiency, increased stability and product quality the direct control of plasma applications is a challenging subject for plasma technology. Therefore, appropriate diagnostic tools are necessary allowing for on-line process monitoring in such applications. Pulsed QCLs are able to emit mid-IR radiation near room temperature. Compared with lead salt lasers, QCLs allow the realization of very compact mid-infrared sources characterized by narrow line width combining single-frequency operation and considerably higher power values, i.e. of tens of mW. The output power is sufficient to combine them with thermoelectrically cooled infrared detectors, which permits a decrease in the apparatus size and gives a unique opportunity to design compact liquid nitrogen-free mid-IR spectroscopic systems. These positive features of quantum cascade laser absorption spectroscopy (QCLAS) can open up new fields of application in research and industry, including studies of gases in atmospheric, environmental and plasma chemistry but also for *in situ* control of industrial plasma processes.

Recently, a compact quantum cascade laser measurement and control system (Q-MACS) has been developed for time-resolved plasma diagnostics, process control and trace gas monitoring [130, 131]. The Q-MACS system contains a tuneable quantum cascade laser which can be directed through a plasma or into a multi-pass cell for exhaust gas detection. Rapid scan software with real-time line shape fitting provides a time resolution up to 1 μs to study kinetic processes of infrared active compounds in plasmas or gases. The Q-MACS-Basic system has been designed as a platform for various applications of QCLAS (figure 29).

Measurements with the Q-MACS-Basic were performed in an industrial pulsed plasma reactor used to deposit boron based hard coatings. Figure 30 shows an absorption spectrum of diborane near 1613 cm^{-1} recorded with 5% admixture of this molecular precursor gas in hydrogen and argon. Using the

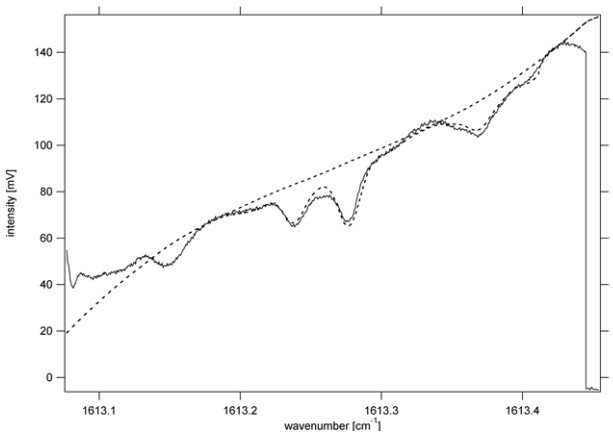

Figure 30. Fitted absorption spectrum of diborane at 1613 cm^{-1} measured in an industrial pulsed DC reactor with 5% diborane at the gas inlet ($p = 200$ Pa) [131].

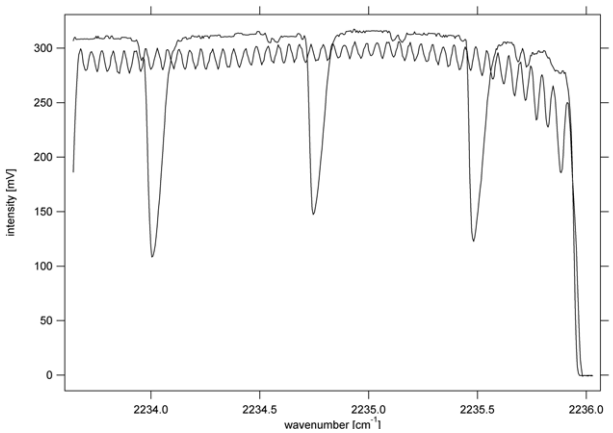

Figure 31. Absorption spectrum of N_2O contained in a reference gas cell ($l = 15$ cm, $p = 6.6$ mbar) at 2235 cm^{-1} and also the etalon pattern of known fringe spacing (fsr $= 0.049$ cm^{-1}) both recorded in a single QCL pulse ($t = 100$ ns) [131].

software package 'TDLWintel' it was possible to continuously monitor the concentration change of diborane while driving a process plasma. The measurement results are not only displayed but can be transferred via hardware interfaces to other systems, e.g. for the use in automated process monitoring and controlling. These measurements prove that QCLAS can be useful for improving the reliability and effectiveness of industrial plasma processes.

The scan through an infrared spectrum can be achieved by a bias dc ramp, in the interpulse mode. Another option is the scanning in single, longer pulses, using the intrapulse mode. An example of a 1.7 cm^{-1} long scan in this mode is shown in figure 31. Since the duty cycle of QCL is about 1 per cent the temporal resolution in this mode can be as good as a few μs. Therefore, it fits very well to measurements of rapidly changing chemical processes.

For high sensitivity trace gas measurements a compact and transportable measurement system, the Q-MACS-Trace, was developed. It combines the Q-MACS-Basic with a 56 m astigmatic multi-pass absorption cell of the Herriot type [132], a compact optical system and a computer system. The sensitivity of the Q-MACS-Trace was as high as a few ppb

Figure 32. Photograph of the Q-MACS-Trace system with optical arrangement and laptop for analysis. (1 channel system with 56 m long path cell, sensitivity: ppb [131].)

(parts per billion—1/10^9). Figure 32 shows a photograph of the Q-MACS-Trace with optical arrangement and laptop for analysis. The Q-MACS-Trace optical system is designed around the QCL laser head.

5. Summary and conclusions

During the past few years a variety of phenomena in molecular non-equilibrium plasmas in which many short-lived and stable species are produced have been successfully studied based on diode laser absorption techniques in the mid-infrared spectral range, with which the present review paper is concerned. It has been possible to determine absolute concentrations of ground states using spectroscopy thereby providing a link with chemical modelling of the plasma, the ultimate objective being to understand better the chemical and reaction kinetic processes occurring in the plasma. In table 1 the major results are shown. The other essential component needed to reach this objective is to determine physical parameters of the plasma, for example, temperatures, degrees of dissociation and dynamics of reaction kinetic processes, and the present paper discusses methods for achieving this. The need for a better scientific understanding of plasma physics and chemistry has stimulated the application of TDLAS, which has been proven to be one of the most versatile techniques for studying molecular plasmas. Based on the recent development of quantum cascade lasers the further spread of this method of high resolution mid-infrared spectroscopy to industrial applications has become a reality.

Table 1. Tabulation of the major results.

Molecular species	Wavenumber region used cm^{-1}	Type of plasma	Concentration range	Gas temperature	Plasma chemistry modelling	References
BH BH_3 B_2H_6	2143.39 2170.039 2596 1583 2596	MW up to 8 mbar $Ar/H_2/B_2H_6$	Relative concentration	1000 K	No	[94]
$^{10}B^{16}O$ $^{11}B^{16}O$	∼1915 ∼1861	MW post-discharge 200 mTorr $N_2/O_2/BCl_3$	Relative concentration	300 K	No	[120, 123]
CF CF_2 CF_3 CF_4	1298 1096 1260 1283	RF up to 500mTorr Ar+CF_4 or CHF_3	Relative concentration	350–400K	No	[9, 12, 14]
CH_3	606–608	ac parallel plate reactor CH_4 or $CH_4/H_2/O_2$	$\sim10^{12}$ cm^{-3}	325 K	Yes	[10, 13]
	606–612	AC glow discharge $[(CH_3)_3CO]_2$ CH_3I $(CH_3)_2CO$ CH_3SH CH_3OH	Relative concentration	400–800 K	No	[15]
	∼606	RF CH_4 diluted in He, Ne, Ar, Kr or Xe	—	—	No	[16–18]
	∼606	RF+MW H_2/CH_3OH	—	—	No	[41, 43]
	∼606	RF 1 mbar CH_4	10^{11}–10^{12} cm^{-3}	∼300–500 K	No	[20]
		RF CH_3OH/H_2O 1 Torr	$\sim10^{12}$ cm^{-3} —		No —	[44]
	606.120 32	RF Ar/HMDSO 0.08–0.6 mbar	$\sim10^{13}$ cm^{-3}	500 K	No	[75]
	∼606	ECR H_2/CH_4 or CH_3OH 1.3 Pa	$\sim10^{11}$ cm^{-3}		No	[42]
	606.120 32	MW $H_2/Ar/N_2$+CH_4 or CH_3OH mixture 1 mbar	10^{12}–10^{13} cm^{-3}	1000 K	Yes	[35, 45]
		MW Surface wave discharge Up to 10 mbar H_2/CH_4	$\sim10^{12}$ cm^{-3}	800–2500 K	No	[62]
	612.413 44	MW Bell–Jar cavity Up to 100 mbar H_2/CH_4	10^{13}–10^{14} cm^{-3}	2000–3500 K	Yes	[35, 38, 68–70, 101]
CH_4	6067	RF 1 mbar CH_4 plasma	$\sim10^{16}$ cm^{-3}	∼300–500 K	No	[20]
	3013.7	RF Ar/HMDSO 0.08–0.6 mbar	$\sim10^{14}$ cm^{-3}	500 K	No	[75]
	1347.054 29 1347.195 15	MW $H_2/Ar/N_2$+CH_4 or CH_3OH mixture 1 mbar	$\sim10^{15}$ cm^{-3}	1000 K	Yes	[45]
	1302.736 2978.848	MW Surface wave discharge Up to 10 mbar H_2/CH_4	10^{15}–10^{16} cm^{-3}	800–2500 K	No	[62]
	1302.4515 2989.9814	MW Bell–Jar cavity Up to 100 mbar H_2/CH_4	10^{15}–10^{16} cm^{-3}	2000–3500 K	Yes	[35, 68–70]

Table 1. Continued.

Molecular species	Wavenumber region used cm^{-1}	Type of plasma	Concentration range	Gas temperature	Plasma chemistry modelling	References
C_2H_2	760–790	ac parallel plate reactor $CH_4/H_2/O_2$	$\sim 10^{13}$ cm^{-3}	325 K	Yes	[13]
		RF CH_3OH/H_2O 1 Torr	$\sim 10^{12}$ cm^{-3}		No	[44]
	700.9004	RF Ar/HMDSO 0.08–0.6 mbar	10^{13}–10^{14} cm^{-3}	500 K	No	[75]
	1347.1631	MW $H_2/Ar/N_2+CH_4$ or CH_3OH mixture 1 mbar	10^{13}–10^{14} cm^{-3}	1000 K	Yes	[45]
	1302.5968	MW Surface wave discharge Up to 10 mbar H_2/CH_4	10^{14}–10^{15} cm^{-3}	800–2500 K	No	[62]
	1302.5968	MW Bell–Jar cavity Up to 100 mbar H_2/CH_4	10^{15}–10^{16} cm^{-3}	2000–3500 K	Yes	[35, 68–70]
C_2H_4	945–960	AC parallel plate reactor $CH_4/H_2/O_2$	$\sim 10^{13}$ cm^{-3}	325 K	Yes	[13]
	947.9829	MW $H_2/Ar/N_2+CH_4$	10^{11}–10^{12} cm^{-3}	1000 K	Yes	[45]
	948.002	or CH_3OH mixture 1 mbar	—	—	—	
	898.2883	MW Surface wave discharge Up to 10 mbar H_2/CH_4	10^{13}–10^{14} cm^{-3}	800–2500 K	No	[62]
	800–820	AC parallel plate reactor $CH_4/H_2/O_2$	$\sim 10^{13}$ cm^{-3}	325 K	Yes	[13]
C_2H_6	2999.5	RF Ar/HMDSO 0.08–0.6 mbar	10^{15}–10^{16} cm^{-3}	500 K	No	[75]
	2993.361	MW $H_2/Ar/N_2+CH_4$	10^{12}–10^{14} cm^{-3}	1000 K	Yes	[45]
	2993.477	or CH_3OH mixture 1 mbar	—	—	—	
	2980.073	MW Surface wave discharge Up to 10 mbar H_2/CH_4	10^{13}–10^{14} cm^{-3}	800–2500 K	No	[62]
	2993.361	MW Bell–Jar cavity Up to 100 mbar H_2/CH_4	10^{14}–10^{15} cm^{-3}	2000–3500 K	Yes	[35, 68–70]
CH_3OH	1020–1045	AC parallel plate reactor $CH_4/H_2/O_2$	$\sim 10^{13}$ cm^{-3}	325 K	Yes	[13]
	1347.572	MW $H_2/Ar/N_2+CH_4$ or CH_3OH mixture 1 mbar	$\sim 10^{15}$ cm^{-3}	1000 K	Yes	[45]
CH_2O	1720–1750	ac parallel plate reactor $CH_4/H_2/O_2$ plasma	$\sim 10^{14}$ cm^{-3}	325 K	Yes	[13]
	1777.3196	MW $H_2/Ar/N_2+CH_4$ or CH_3OH mixture 1 mbar	$\sim 10^{12}$ cm^{-3}	1000 K	Yes	[45]
C_2N_2	2149.990 48	MW $H_2/Ar/N_2+CH_4$ or CH_3OH mixture 1 mbar	10^{11}–10^{12} cm^{-3}	1000 K	Yes	[45]
CO	2050–2150	ac parallel plate reactor	$\sim 10^{14}$ cm^{-3}	325 K	Yes	[13]

Table 1. Continued.

Molecular species	Wavenumber region used cm^{-1}	Type of plasma	Concentration range	Gas temperature	Plasma chemistry modelling	References
CO_2	600–620	$CH_4/H_2/O_2$	$\sim10^{14}$ cm^{-3}			
CO	2060	RF 1 mbar	$\sim10^{14}$–10^{15} cm^{-3}	~300–500 K	No	[20]
CO_2	2250	CH_4/O_2	$\sim10^{14}$–10^{15} cm^{-3}			
HCOOH	1720–1750	ac parallel plate reactor $CH_4/H_2/O_2$ plasma	$\sim10^{13}$ cm^{-3}	325 K	Yes	[13]
HCN	785.3894 785.576 66	MW $H_2/Ar/N_2$+CH_4 or CH_3OH mixture 1 mbar	10^{14}–10^{15} cm^{-3}	1000 K	Yes	[45]
NH_3	948.232 06	MW $H_2/Ar/N_2$+CH_4 or CH_3OH mixture 1 mbar	10^{13}–10^{14} cm^{-3}	1000 K	Yes	[45]
NO	1880	Pulsed MW 800 mbar $N_2/O_2/C_5H_{10}O$	100–2000 ppm	1000 K	No	[84]
Si_2^-	740–820	AC glow discharge H_2/SiH_4	Relative concentration	—	No	[22]
SiH_3^+	730–1015					[23]

Acknowledgments

This work was partly supported by (a) the Deutsche Forschungsgemeinschaft, Sonderforschungsbereich 198 and Transferbereich 36, (b) the Bundesministerium für Bildung und Forschung, FKZ 13N7451/8, (c) the Deutscher Akademischer Austauschdienst and EGIDE as part of the French–German PROCOPE Collaboration Program (Project 04607QB) and (d) in the framework of the German–Russian–French Trilateral Cooperation Project of University of Greifswald, St Petersburg State University and University of Paris-South. The authors convey their sincere thanks to all present and former members of the laboratories involved in Greifswald, Paris and Cambridge for permanent support and a stimulating scientific climate. In particular, the authors are indebted to all co-authors of former papers whose contributions made the present review possible.

References

[1] Mechold L 2000 *PhD Thesis* University of Greifswald, Germany (Berlin: Logos)
[2] Demtröder W 2002 *Laser Spectroscopy: Basic Concepts and Instrumentation* (Berlin: Springer)
[3] Duxbury G 2000 *Infrared Vibration–Rotation Spectroscopy; From Free Radicals to the Infrared Sky* (Chichester: Wiley)
[4] Tittel F K, Richte D and Freed A 2003 Mid-infrared laser applications in spectroscopy *Solid State Infrared Sources* ed I T Sorokina and K L Vodopyanov p 445 (Berlin Heidelberg: Springer)
[5] Romanini D and Lehmann K K 1993 *J. Chem. Phys.* **99** 6287
[6] Romanini D, Kachanov A A, Sadeghi N and Stoeckel F 1997 *Chem. Phys. Lett.* **264** 316
[7] Campargue A, Romanini D and Sadeghi N 1998 *J. Phys. D: Appl. Phys.* **31** 1168
[8] Kotterer M, Conceicao J and Maier J P 1996 *Chem. Phys. Lett.* **259** 233
[9] Haverlag M, Stoffels E, Stoffels W W, Kroesen G M W and de Hoog F J 1996 *J. Vac. Sci. Technol.* A **14** 380
[10] Davies P B and Martineau P M 1992 *Adv. Mater.* **4** 729
[11] Naito S, Ito N, Hattori T and Goto T 1995 *Japan. J. Appl. Phys.* **34** 302
[12] Haverlag M, Stoffels E, Stoffels W W, Kroesen G M W and de Hoog F J 1994 *J. Vac. Sci. Technol.* A **12** 3102
[13] Röpcke J, Mechold L, Käning M, Fan W Y and Davies P B 1999 *Plasma Chem. Plasma Process.* **19** 395
[14] Haverlag M, Stoffels E, Stoffels W W, Kroesen G M W and de Hoog F J 1996 *J. Vac. Sci. Technol.* A **14** 384
[15] Yamada C and Hirota E 1983 *J. Chem. Phys.* **78** 669
[16] Naito S, Ikeda M, Ito N, Hattori T and Goto T 1993 E *Japan. J. Appl. Phys.* **32** 5721
[17] Naito S, Ito N, Hattori T and Goto T 1994 *Japan. J. Appl. Phys.* **33** 5967
[18] Ikeda M, Ito N, Hiramatsu M, Hori M and Goto T 1997 *J. Appl. Phys.* **82** 4055
[19] Kroesen G M W, den Boer J H W G, Boufendi L, Vivet F, Khouli K, Bouchoule A and de Hoog FV 1996 *J. Vac. Sci. Technol*. A **14** 546
[20] Busch C, Möller I and Soltwisch H 2001 *Plasma Sources Sci. Technol*. **10** 250
[21] Serdioutchenko A, Möller I and Soltwisch H 2004 *Spectrochim. Acta* A **60** 3311
[22] Liu Z and Davies P B 1996 *J. Chem. Phys.* **105** 3443
[23] Davies P B and Smith D M 1994 *J. Chem. Phys*. **100** 6166
[24] Röpcke J, Mechold L, Käning M, Anders J, Wienhold F G, Nelson D and Zahniser M 2000 *Rev. Sci. Instrum.* **71** 3706
[25] McManus J B, Nelson D, Zahniser M, Mechold L, Osiac M, Röpcke J and Rousseau A 2003 *Rev. Sci. Instrum.* **74** 2709
[26] Sugai H, Kojima H, Ishida A and Toyoda H 1990 *Appl. Phys. Lett.* **56** 2616
[27] Sugai H and Toyoda H 1992 *J. Vac. Sci Technol.* A **8** 1193
[28] Zarrabian M, Leteinturier C and Turban G 1998 *Plasma Sources Sci. Technol.* **7** 607
[29] Zalicki P, Ma Y, Zare R N, Wahl, E H, Dadamio J R, Owano T G and Kruger C H 1995 *Chem. Phys. Lett.* **234** 269
[30] Zalicki P, Ma Y, Zar R N, Wahl E H, Dadamio J R, Owano T G and Kruger C H 1995 *Appl. Phys. Lett.* **67** 144
[31] Wahl E H, Owano T G, Kruger C H, Zalicki P, Ma Y and Zare R N 1997 *Diamond. Relat. Mater.* **6** 476

[32] Childs M A, Menningen K L, Chevako P, Spellmeyer N W, Anderson L W and Lawler J E 1992 *Phys. Lett.* A **171** 87
[33] Menningen K L, Childs M A, Chevako P, Toyoda H, Anderson L W and Lawler J 1993 *Chem. Phys. Lett.* **204** 573
[34] Menningen K L, Childs M A, Toyoda H, Ueda Y, Anderson L W and Lawler J E 1994 *Diamond. Relat. Mater.* **3** 422
[35] Lombardi G, Stancu G D, Hempel F, Gicquel A and Röpcke J 2004 *Plasma Sources Sci. Technol.* **13** 27
[36] Wormhoudt J 1990 *J. Vac. Sci. Technol.* A **8** 1722
[37] Wormhoudt J and McCurdy K E 1989 *Chem. Phys. Lett.* **156** 47
[38] Stancu G D, Röpcke J and Davies P B 2005 *J. Chem. Phys.* **122** 014306
[39] Davies P B and Martineau P M 1990 *Appl. Phys. Lett.* **57** 237
[40] Davies P B and Martineau P M 1992 *J. Appl. Phys.* **71** 6125
[41] Naito S, Ito N, Hattori T and Goto T 1995 *Japan. J. Appl. Phys.* **34** 302
[42] Ikeda M, Aiso K, Hori M and Goto T 1995. *Japan. J. Appl. Phys.* **34** 3273
[43] Ikeda M, Hori M, Goto T, Inayoshi M, Yamada K, Hiramatsu M and Nawata M 1995 *Japan. J. Appl. Phys.* **34** 2484
[44] Kim S, Billesbach D P and Dillon R 1997 *J. Vac. Sci. Technol.* A **15** 2247
[45] Hempel F, Davies P B, Loffhagen D, Mechold L and Röpcke J 2003 *Plasma Sources Sci. Technol.* **12** S98
[46] Ohl A 1998 *J. Phys.* IV **8** 83
[47] Vandevelde T, Nesladek M, Quaeyhaegens C and Stals L 1997 *Thin Solid Films* **308–309** 154
[48] Vandevelde T, Wu T D, Quaeyhaegens C, Vlekken J, D'Olieslaeger M and Stals L 1999 *Thin Solid Films* **340** 159
[49] Mutsukura N 2001 *Plasma Chem. Plasma Process.* **21** 265
[50] Bhattacharyya S, Granier A and Turban G 1999 *J. Appl. Phys.* **86** 4668
[51] Zhang M, Nakayama Y, Miyazaki T and Kume M 1998 *J. Appl. Phys.* **85** 2904
[52] Dinescu G, De Graaf A, Aldea E, and van de Sanden M C M 2001 *Plasma Sources Sci. Technol.* **10** 513
[53] De Graaf A, Aldea E, Dinescu G and van de Sanden M C M 2001 *Plasma Sources Sci. Technol.* **10** 524
[54] Penetrante B M, Hsiao M C, Bardsley J N, Merritt B T, Vogtlin G E, Kuthi A, Burkhart C P and Bayless J R 1997 *Plasma Sources Sci. Technol.* **6** 251
[55] Kareev M, Sablier M and Fujii T 2000 *J. Phys. Chem.* **104** 7218
[56] Coll P, Coscia D, Gazeau M C, De Vanssay E, Guillemin J C and Raulin F 1995 *Adv. Space Res.* **16** 93
[57] De Vanssay E, Gazeau M C, Guillemin J C and Raulin F 1995 *Planet. Space Sci.* **43** 25
[58] Tabares F L, Tafalla D, Tanarro I, Herrero V J, Islyaikin A and Maffiotte C 2002 *Plasma Phys. Control. Fusion* **44** L37
[59] White J U 1942 *J. Opt. Soc. Am.* **32** 285
[60] Gemini Scientific Instruments 2001 *Multi-Pass Optics Alignment Instructions* (Manual) www.gascell.com
[61] Fan W Y, Knewstubb P F, Käning M, Mechold L, Röpcke J and Davies P B 1999 *J. Phys. Chem.* A **103** 4118
[62] Mechold L, Röpcke J, Duten X and Rousseau A 2001 *Plasma Sources Sci. Technol.* **10** 52
[63] Loffhagen D and Winkler R 1996 *J. Phys. D: Appl. Phys.* **29** 618
[64] Buckman S J and Phelps A V 1985 *J. Chem. Phys.* **82** 4999
[65] Phelps A V and Pitchford L C 1985 *Phys. Rev.* **31** 2932
[66] Gruen D M, Pan X, Krauss A R, Liu S, Luo J and Foster C M 1994 *J. Vac. Sci Technol.* A **12** 1491
[67] Bénédic F, Assouar M B, Mohasseb F, Elmazria O, Alnot P and Gicquel A 2004 *Diamond Relat. Mater.* **13** 347
[68] Lombardi G, Hassouni K, Bénédic F, Mohasseb F, Röpcke J and Gicquel A 2004 *J. Appl. Phys.* **96** 6739
[69] Lombardi G, Hassouni K, Stancu G D, Mechold L, Röpcke J and Gicquel A 2005 *Plasma Sources Sci. Technol.* **14** 440
[70] Lombardi G, Hassouni K, Stancu G D, Mechold L, Röpcke J and Gicquel A 2005 *J. Appl. Phys.* **98** 053303
[71] Bugaev SP, Kozyrev A V, Kushinov V A, Sochugov N S and Khryapov P A 1998 *Plasma Chem. Plasma Process.* **18** 247
[72] Hsieh L-T, Lee W-J, Chen C-Y, Chang, M-B and Chang H-C 1998 *Plasma Chem. Plasma Process.* **18** 215
[73] Wrobel A M and Wertheimer M R 1990 Plasma-polymerized organosilicones and organometallics *Plasma Deposition, Treatment and Etching of Polymers* ed R d' Agostino (San Diego: Academic) p 163
[74] Röpcke J, Ohl A and Schmidt M 1993 *J. Anal. At. Spectrom.* **8** 803
[75] Röpcke J, Revalde G, Osiac M, Li K and Meichsner J 2002 *Plasma Chem. Plasma Process.* **22** 137
[76] Schmidt M 1973 *Beitr. z. Plasma Phys.* **13** 347
[77] Foest R, Schmidt M, Hannemann M and Basner R 1994 On the ions in an argon-hexamethyldisiloxane radio-frequency-discharge *Gaseous Dielectrics VII* ed L G Christophorou and D R James (New York: Plenum) p 335
[78] Van Veldhuizen E M (ed) 2000 *Electrical Discharges for Environmental Purposes Fundamentals and Applications* (Huntington, NY: NOVA Science Publishers)
[79] Penetrante B 1993 *Non-Thermal Plasma Techniques for Pollution Control* (NATO ASI Series) vol G34, ed S Schultheis (Berlin: Springer)
[80] Yamamoto T 1997 *J. Electrostat.* **42** 227
[81] Filimonova E, Amirov R, Kim H and Park I 2000 *J. Phys. D: Appl. Phys.* **33** 1716
[82] Mc Adams J 2001 *J. Phys. D: Appl. Phys.* **34** 2810
[83] Filimonova E, Kim Y-H, Hong S, Han S-Y and Song Y-H 2001 *Proc. 15th Int. Symp. Plasma Chem. (Orléans, France)* p 3041
[84] Rousseau A, Dantier A, Gatilova L V, Ionikh Y, Röpcke J and Tolmachev Y A 2005 *Plasma Sources Sci. Technol.* **14** 70
[85] Albella J M, Gomez-Aleixandre C, Sanchez-Garrido O, Vazquez L and Martinez-Duart J M 1995 *Surf. Coat. Technol.* **70** 163
[86] Andujar J L, Bertran E and Polo M C 1998 *J. Vac. Sci. Technol.* **16** 578
[87] Franz D, Hollenstein M and Hollenstein C 2000 *Thin Solid Films* **379** 37
[88] Ichiki T, Momose T and Yoshida T 1994 *J. Appl. Phys.* **75** 1330
[89] Ichiki T and Yoshida T 1994 *Appl. Phys. Lett.* **64** 851
[90] Gonon P, Deneuville A, Fontaine F, Gheeraert E, Campargue A, Chenevier M and Rodolphe S 1995 *J. Appl. Phys.* **78** 7404
[91] Kawaguchi K, Butler J E, Yamada C, Bauer S H, Minowa T, Kanamori H and Hirota E 1987 *J. Chem. Phys.* **87** 2438
[92] Kawaguchi K 1992 *J. Chem. Phys.* **96** 3411
[93] Pianalto F S, O'Brien L C, Keller P C and Bernath P F 1988 *J. Mol. Spectrosc.* **129** 348
[94] Lavrov B P, Osiac M, Pipa A V and Röpcke J 2003 *Plasma Sources Sci. Technol.* **12** 576
[95] Arthur N L 1986 *J. Chem. Soc. Faraday Trans. II* **82** 331
[96] Davidson D F, Chang A Y, Di Rosa M D and Hanson R K 1993 *J. Quant. Spectrosc. Radiat. Transfer* **49** 559
[97] Gicquel A, HassouniK, Owano T, DutenX, and Cappelli M 1999 *6th Int. Symp. on Diamond Material (Electrochem. Society Proc.) (Honolulu)* vol 99–32 p 41
[98] Glänzer K, Quack M and Troe J 1977 *16th Int. Symp. on Combustion* (Pittsburgh: The Combustion Institute) p 949
[99] Zahniser M S, Nelson D D and Kolb C E 2002 *Applied Combustion Diagnostics* ed K Kohse-Hoinghaus and J Jeffries (New York: Taylor and Francis) p 648

[100] Nelson D D, Shorter J H, McManus J B and Zahniser M S 2002 *Appl. Phys.* B **75** 343
[101] Stancu G D 2004 *PhD Thesis* University of Greifswald, Germany
[102] Bézard B, Feuchtgruber H, Moses J I and Encrenaz T 1998 *Astro. Astrophys.* **334** L41
[103] Bezard B, Romani P N, Feuchtgruber H and Encrenaz T 1999 *Astrophys. J.* **515** 868
[104] Feuchtgruber H, Helmich F P, van Dishoeck E F and Wright C M 2000 *Astrophys. J.* **535** L111
[105] Laguna G A and Baughcum S L 1982 *Chem. Phys. Lett.* **88** 568
[106] Cody R J, Payne Jr W A, Thorn Jr R P, Nesbitt F L, Iannone M A, Tardy D C and Stief L 2002 *J. Phys. Chem.* A **106** 6060
[107] Walter D, Grotheer H H, Davies J W, Pilling M J and Wagner A F 1990 *23rd Symp. on Combustion* p 107
[108] Macpherson M T, Pilling M J and Smith M J C 1983 *Chem. Phys. Lett.* **94** 430
[109] Macpherson M T, Pilling M J and Smith M J C 1985 *J. Phys. Chem.* **89** 2268
[110] Slagle I R, Gutman D, Davies J W and Pilling M J 1988 *J. Phys. Chem.* **92** 2455
[111] Wagner A F and Wardlaw D M 1988 *J. Phys. Chem.* **92** 2462
[112] Callear A B and Metcalfe M P 1976 *Chem. Phys.* **14** 275
[113] Baulch D L *et al* 1994 *J. Phys. Chem. Ref. Data* **23** 980
[114] Schwarz S, Rosiwal S M, Frank M, Breidt D and Singer R F 2002 *Diamond Relat. Mater.* **11** 589
[115] Hunt N T, Röpcke J and Davies P B 2000 *J. Mol. Spectrosc.* **204** 120
[116] Mulliken R S 1925 *Phys. Rev.* **25** 259
[117] Coxon J A, Foster S C and Naxakis S 1984 *J. Mol. Spectrosc.* **105** 465
[118] Mélen F, Dubois I and Bredohl H 1985 *J. Phys. B: At. Mol. Phys.* **18** 2423
[119] Tanimoto M, Saito S and Hirota E 1986 *J. Chem. Phys.* **84** 1210
[120] Osiac M, Röpcke J and Davies P B 2001 *Chem. Phys. Lett.* **344** 92
[121] Clyne M A A and Heaven M C 1980 *Chem. Phys.* **51** 299
[122] Llewellyn I P, Fontijn A and Clyne M A A 1981 *Chem. Phys. Lett.* **84** 504
[123] Stancu G D, Röpcke J and Davies P B 2004 *J. Mol. Spectrosc.* **223** 181
[124] Rehfuss B D, Suh M H, Miller T A and Bondybey V E 1992 *J. Mol. Spectrosc.* **151** 437
[125] Prasad C V V, Bernath P F, Frum C and Engleman R 1992 *J. Mol. Spectrosc.* **151** 459
[126] Hübner M, Castillo M, Davies P B and Röpcke J 2005 *Spectrochim. Acta A Mol. Spectrosc.* **61** 57
[127] Röpcke J 2000 *Acta Phys. Univ. Comen.* **XLI** 87
[128] Röpcke J, Mechold L, Duten X and Rousseau A 2001 *J. Phys. D: Appl. Phys.* **34** 2336
[129] Schulz-von der Gathen V, Röpcke J, Gans T, Käning M, Lukas C and Döbele H F 2001 *Plasma Sources Sci. Technol.* **10** 530
[130] Hempel F, Glitsch S, Röpcke J, Saß S and Zimmermann H 2005 On the measurement of absolute plasma species densities using quantum cascade laser-absorption spectroscopy *Plasma Polymers and Related Materials* ed M Mutlu (Ankara: Hacettepe University Press) p 142
[131] Röpcke J, Glitsch S, Hempel F, Sass S, Schulz K-D, Weltmann K-D and Zimmermann H 2005 *Proc. 48th Annual SVC Conf. (Denver, USA)* p 54
[132] McManus J B, Kebabian P L and Zahniser M S 1995 *Appl. Opt.* **34** 3336
[133] Lancaster D G, Richter D, and Tittel F K 1999 *Appl. Phys.* B **69** 459
[134] Rehle D, Leleux D, Erdely M, Tittel F K, Fraser M and Friedfeld S 2001 *Appl. Phys.* B **72** 947